ERDC TR-20-25

US Army Corps of Engineers®
Engineer Research and Development Center

ERDC
ENGINEER RESEARCH & DEVELOPMENT CENTER

Future Investment Fund

Evaluating the Conductive Properties of Melanin-Producing Fungus, *Curvularia lunata*, after Copper Doping

Robert M. Jones, Eftihia V. Barnes, Alison K. Thurston, and Robyn A. Barbato

October 2020

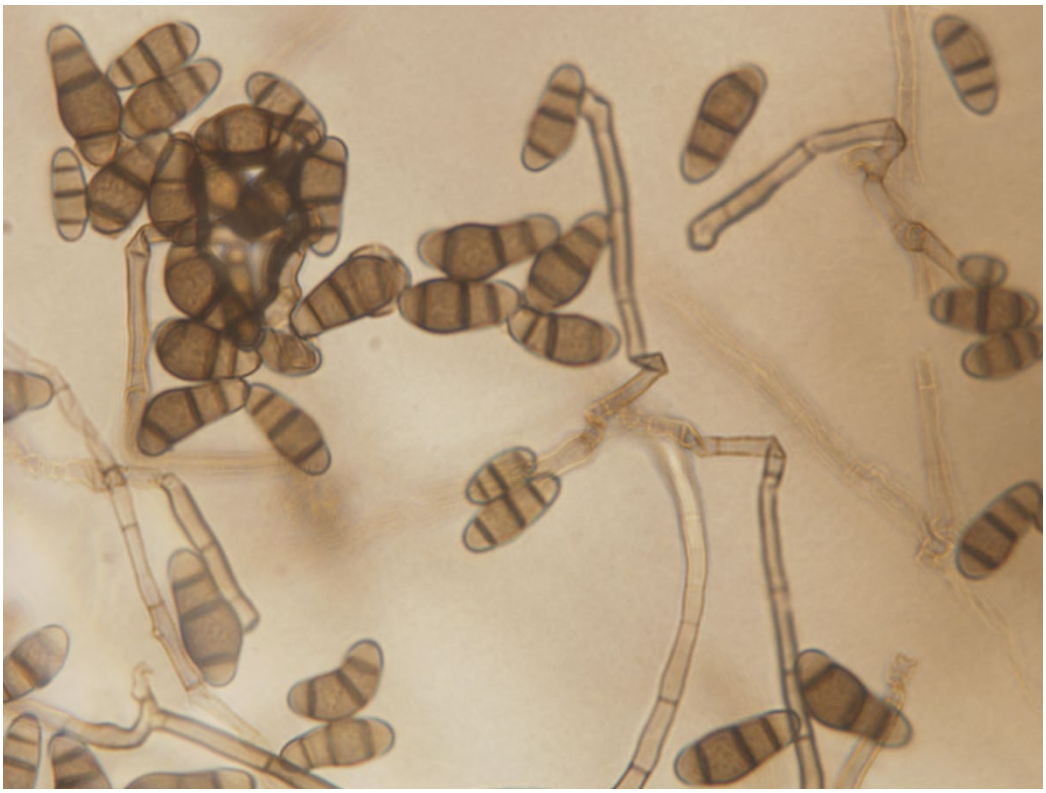

Engineer Research and Development Center

The U.S. Army Engineer Research and Development Center (ERDC) solves the nation's toughest engineering and environmental challenges. ERDC develops innovative solutions in civil and military engineering, geospatial sciences, water resources, and environmental sciences for the Army, the Department of Defense, civilian agencies, and our nation's public good. Find out more at www.erdc.usace.army.mil.

To search for other technical reports published by ERDC, visit the ERDC online library at https://erdclibrary.on.worldcat.org/discovery.

ERDC TR-20-25
October 2020

Evaluating the Conductive Properties of Melanin-Producing Fungus, *Curvularia lunata*, after Copper Doping

Robert M. Jones, Alison K. Thurston, and Robyn A. Barbato

U.S. Army Engineer Research and Development Center (ERDC)
Cold Regions Research and Engineering Laboratory (CRREL)
72 Lyme Road
Hanover, NH 03755-1290

Eftihia V. Barnes

U.S. Army Engineer Research and Development Center (ERDC)
Geotechnical and Structures Laboratory (GSL)
Waterways Experiment Station, 3909 Halls Ferry Road
Vicksburg, MS 39180-6199

Final Report

Prepared for Engineer Research and Development Center
3909 Halls Ferry Road
Vicksburg, MS 39180

Under Future Investment Fund, Funding Account Number U4373350

Abstract

Melanins are pigmented biomacromolecules found throughout all domains of life. Of melanins' many unique properties, their malleable electrically conductive properties and their ability to chelate could allow them to serve as material for bioelectronics. Studies have shown that sheets or pellets of melanin conduct low levels of electricity; however, electrical conductance of melanin within a cellular context has not been thoroughly investigated. In addition, given the chelating properties of melanin, it is possible that introducing traditionally conductive metal ions could improve the conductivity.

Therefore, this study investigated the conductive properties of melanized cells and how metal ions change these. We measured the conductivity of pulverized *Curvularia lunata,* a melanized filamentous fungi, with and without the addition of copper ions. We then compared the conductivity measurements of the fungus to chemically synthesized, commercially bought melanin.

Our data showed that the conductivity of the melanized fungal biomass was an order of magnitude higher when grown in the presence of copper. However, it was two orders of magnitude less than that of synthetic melanin. Interestingly, conductance was measurable despite additional constituents in the pellet that may inhibit conductivity. Therefore, these data show promising results for using melanized cells to carry electrical signals.

Contents

Figures and Tables

Figures

Tables

Preface

This study was conducted for the U.S. Army Engineer Research and Development Center (ERDC), under the Future Investment Fund, Funding Account Number U4373350.

The work was performed by the Biogeochemical Sciences Branch of the Research and Engineering Division, ERDC Cold Regions Research and Engineering Laboratory (CRREL). At the time of publication, Dr. Steven E. Peckham was Acting Branch Chief; and Mr. J. D. Horne was the Division Chief. The Deputy Director of ERDC-CRREL was Mr. David B. Ringelberg, and the Director was Dr. Joseph L. Corriveau.

And the work was performed by the Structural Mechanics Branch of the Geosciences and Structures Division, ERDC Geotechnical and Structures Laboratory (GSL). At the time of publication, Mr. Bradford A. Steed was Branch Chief; and Mr. James L. Davis was Division Chief. The Deputy Director of ERDC-GSL was Mr. Charles W. Ertle II, and the Director was Mr. Bartley P. Durst.

COL Teresa A. Schlosser was Commander of ERDC, and Dr. David W. Pittman was the Director.

Acronyms and Abbreviations

CRREL	Cold Regions Research and Engineering Laboratory
ERDC	Engineer Research Development Center
GSL	Geotechnical and Structures Laboratory
MEA	Malt Extract Agar
MEB	Malt Extract Broth
PDA	Potato Dextrose Agar
PDB	Potato Dextrose Broth
RPM	Rotations per Minute
SEM	Scanning Electron Microscope
SMU	Source Meter Unit
tPDB	Thickened Potato Dextrose Broth
tMEB	Thickened Malt Extract Broth
UV	Ultraviolet
YEPDxyl	Yeast Extract Peptone D-xylose Broth
YMA	Yeast Malt Agar
YMB	Yeast Malt Broth

1 Introduction

1.1 Background

1.1.1 Melanin: properties and sources

Melanin, an umbrella term encapsulating a diverse family of pigmented biomacromolecules, performs several biological functions in organic life (Meredith and Sarna 2006). However, melanins as a group, due to insolubility, are resistant to many traditional biochemical techniques necessary to define chemical structure. Thus, there is still a lack of a consensus on unifying properties of melanins (Eisenman and Casadevall 2012; d'Ischia et al. 2013). Without further resolution melanin molecules, in general, have been found to have the following common characteristics: formation through the oxidation and polymerization of tyrosine, dopamine, and or phenols, high molecular weight, resistance to acids, and an overall negative charge (Riley 1997; Schmaler-Ripcke et al. 2009; d'Ischia et al. 2013; Solano 2014; Ambrico et al. 2015).

Melanin can be found in animals, plants, bacteria, and fungi. There are three primary types of melanin found in nature: eumelanin, pheomelanin, and neuromelanin (Figure 1) (d'Ischia et al. 2013; Solano 2014). Additionally, melanin can be produced through chemical synthesis via the oxidation of various precursors, such as L-tyrosine and L-dopa (d'Ischia et al. 2013). Of the natural melanins, eumelanin is the most common and is characterized by its dark brown to black appearance (Micillo et al. 2016). Eumelanins serve many biological functions, though primarily they aid in mitigating the effects of free radicals and provide ultraviolet (UV) protection (Meredith and Sarna 2006). Pheomelanin appears as a yellow to red pigment that is chemically distinctive from eumelanin as it incorporates benzothiazine and benzothiazole units as opposed to the dihydroxyindole-2-carboxylic acid and dihydroxyindole units found in eumelanin (Micillo et al. 2016). Neuromelanin has some structural similarities to both eumelanin and pheomelanin and, like eumelanin, possesses the ability to mitigate free radicals (Haining and Achat-Mendes 2017); however, neuromelanin is found only in neurons within the brain (Graham 1979; El-Naggar and El-Ewasy 2017).

Figure 1. Proposed Structures of Primary Types of Melanin: (*A*) eumelanin, (*B*) pheomelanin, and (*C*) neuromelanin. *Arrows* indicate potential attachment sites to other melanin molecules. (Adapted from Ito and Wakamatsu 2008.)

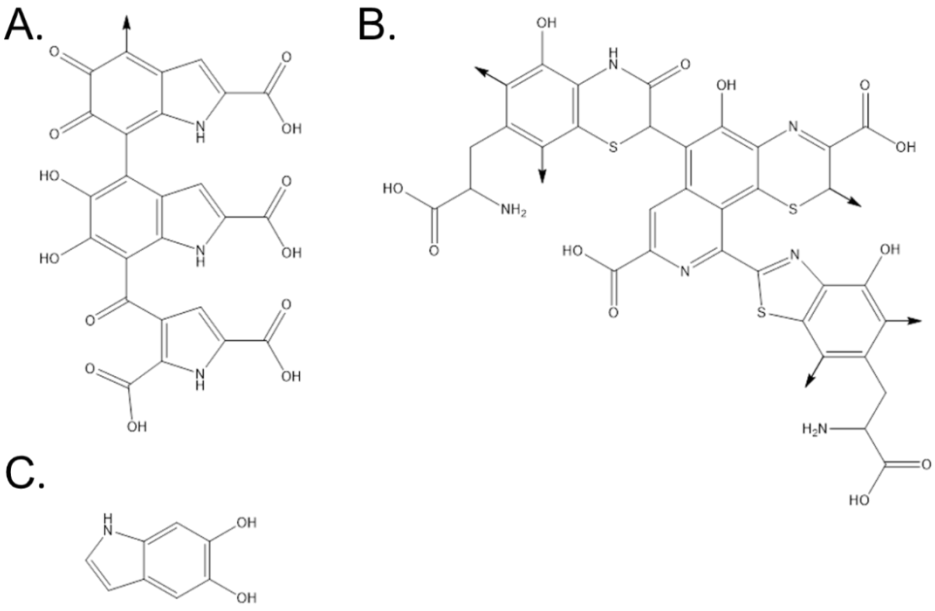

The roles that melanins play in organisms are still under investigation, including metal chelation (Meredith and Sarna 2006), radiation and radionuclide protection (Kunwar et al. 2012), photoreception and photoconductivity (Jeffery et al. 1994; Capozzi et al. 2006), tensile strength (Roy and Rhim 2019), optical tunability (Wang et al. 2018), supercapacitor properties (Kumar et al. 2016), and electrical conductance (Jastrzebska et al. 1996; Mostert, Powell, Pratt, et al. 2012; Mostert, Powel, Gentle, et al. 2012; McGinness et al. 1974) (Figure 2).

Figure 2. Observed functional properties of melanins.

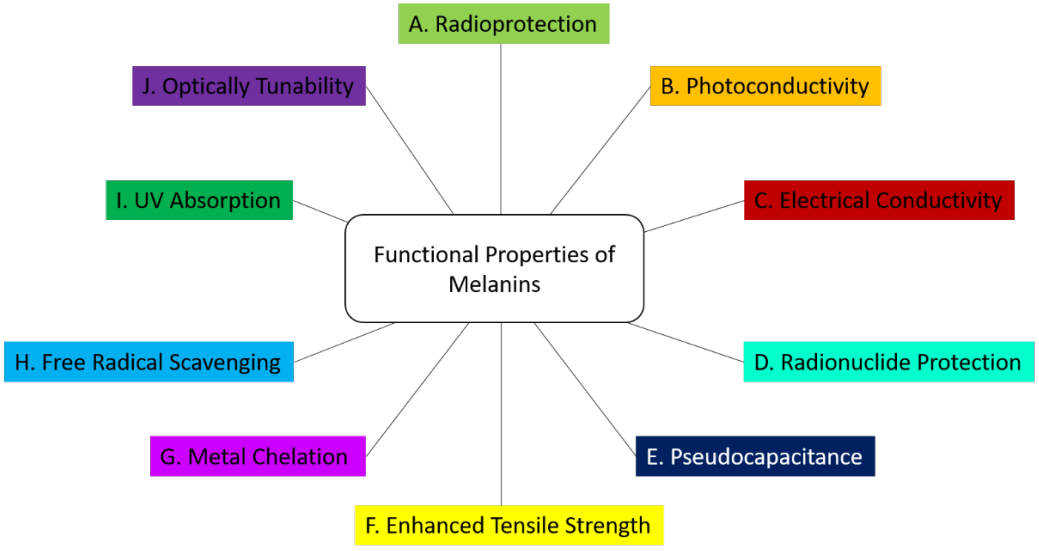

1.1.2 The conductive properties of melanin

Several naturally occurring biomolecules have demonstrated conductive properties, such as DNA strands (Fink and Schonenberger 1999; Rakitin et al. 2001; Waleed et al. 2010); protein structures, like nanowires (Waleed et al. 2010; Rakshit and Mukhopadhyay 2012; Ordinario et al. 2014; Lovley and Walker 2019); and peptide networks (Ashkenasy et al. 2006; Takahashi et al. 2007; Waleed et al. 2010; Ing et al. 2018). However, melanin is unique as it has tunable conductive properties primarily controlled by its hydration state (Jastrzebska et al. 1996, Wunsche et al. 2015) and the method of polymerization (Solano 2014; Ambrico et al. 2015). Furthermore, melanin can exchange both ionic charge and electronic charge, a behavior known as hybrid ionic-electronic conductance (Meredith and Sarna 2006; Ambrico et al. 2015, Barra et al. 2016). This could potentially allow melanin to translate electronic charge to a more biologically relevant ionic charge and vice versa (Barra et al. 2016; Paulsen et al. 2020), which would be key to developing bioelectronics compatible with organisms (Ambrico et al. 2015; Barra et al. 2016).

Melanin, specifically eumelanin, is theorized to gain its conductive properties through the process of self-doping, or the ability to produce charge and charge carriers from interactions between melanin species of different oxidation states (Mostert, Powell, Pratt, et al. 2012; Sheliakina et al. 2018). When the two melanin molecules undergo redox, free radicals and protons are generated, allowing for the transfer of charge (Figure 3) (Meredith and Sarna 2006; Mostert et al. 2016). Because the transfer of charge commonly occurs between water molecules and melanin molecules, the resulting conductivity of melanin is primarily influenced by hydration state (Jastrzebska et al. 1996; Meredith and Sarna 2006); but temperature, and structure also play a crucial role (Meredith and Sarna 2006; Motovilov et al. 2019) and together potentially allow the conductance to be controllable.

Figure 3. Melanin self-doping reaction. Different melanin moieties interact with water to produce charged moieties and hydronium. (Adapted from Sheliakina et al. 2017.)

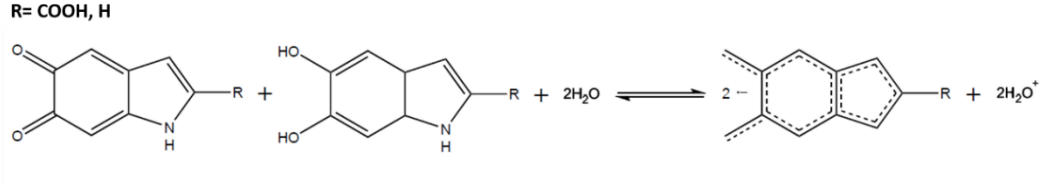

Early research into the conductivity of melanin established a conductive range between 10^{-13} and 10^{-5} S/cm* (McGinness et al. 1974; Jastrzebska et al. 1996). However, modification of the melanin super structure through high-temperature vacuum annealing increased the conductivity of melanin to 300 S/cm (Migliaccio et al. 2019). Apart from demonstrating the efficacy of melanin to act as a practical conductor, Migliaccio et al. (2019) also demonstrated how crucial the formation and structure of melanin granules is to conductivity as the annealing process transformed the granules to a more sheet-like super structure (Migliaccio et al. 2019). While this more extreme process of melanin transformation increased conductivity, Madkhali et al. (2019) showed that metal ions, specifically Fe, Cu, and Zn, can favorably alter the electrochemical properties of melanin.

Overall, the current state of research has demonstrated that the conductivity of melanin can be elevated to levels comparable to other commonly used conductors (based on a traditionally defined range of semiconductance [10^{-5} to 10^{3} S/cm] to conductance [>10^{4} S/cm] [Matijasevic and Brandt 2009]). Furthermore, the conductivity can be potentially be tuned depending on the polymerization (Jastrzebska et al. 1998; Solano 2014; Ambrico et al. 2015) and hydration state (Jastrzebska et al. 1996).

1.1.3 Melanin in fungus

In fungi, melanin is produced utilizing the 1,8-dihydroxynaphthalene pathway (Casadevall et al. 2000; Langfelder et al. 2003; Pal et al. 2014) or the L-3, 4-dihydroxyphenylalanine pathway (Bell and Wheeler 1986; Casadevall et al. 2000; Pal et al. 2014). Melanin molecules are synthesized in a membrane-bounded vesicle called a melanosome and are either directly integrated into the cell wall in layers or excreted (Eisenman and Casadevall 2012; Nosanchuk et al. 2015; Camacho et al. 2019). In some cases, the accumulated melanin can form a sheath or rind external to the cell wall (Butler et al. 2009). The distribution, quantity of melanin, and strategies for incorporation into or around the cell wall in fungi depends on the species; for example, *Aspergillus fumigatus* excretes melanin, which then binds in thin layers to hyphal walls (Heinekamp et al. 2013) whereas *Cryptococcus neoformans* produces melanin and deposits it in

* For a full list of the spelled-out forms of the units of measure and chemical elements used in this document, please refer to *U.S. Government Publishing Office Style Manual*, 31st ed. (Washington, DC: U.S Government Publishing Office, 2016), 248–252, 265, https://www.govinfo.gov/content/pkg/GPO-STYLEMANUAL-2016/pdf/GPO-STYLEMANUAL-2016.pdf.

concentric layers within the cell wall (Nosanchuk et al. 2015). When incorporated as a layer in or on the cell wall, the melanin has been theorized to function as an impermeable boundary as a defense against bacteria, other fungi, and predatory microbes (Morris-Jones et al. 2003, 2005; Nosanchuk et al. 2015). Although the melanin layer is not entirely impermeable, as nuclear magnetic resonance cyroporometry has shown the melanin layer to have selective sized pores potentially for macromolecule transport (Nosanchuk and Casadevall 2006). Though the distribution of melanin in fungi is heterogeneous across species, the most common formation of melanin granules is as stacked planar sheets (Eisenman and Casadevall 2012; Casadevall et al. 2012). It is predicted that melanin functions as scaffolding material, providing additional structural stability to the cell wall and allowing for more structurally complex construction of chitin (Nosanchuk et al. 2015; Cordero and Casadevall 2017).

The purpose of melanin in fungi is theorized to be similar to the role melanin plays other organisms in that it is primarily a protectant against various environmental hazardous specifically radiation (Dadachova et al. 2007, 2008; Eisenman and Casadevall 2012). Recent research of fungal melanin has shown it is a protectant against UV, thermal, and high-energy (specifically gamma) radiation (Turick et al. 2011). In fact, studies have demonstrated that melanin may be involved in radiotrophism (growth towards radiation) and radiosynthesis (consumption of radiation) (Dadachova et al. 2008). Also, in regard to protection, melanin has been demonstrated to be an effective binder of many molecules (Bruenger et al. 1967); however, it has a particular affinity for chelating heavy metal ions (Bruenger et al. 1967; Gadd 1984; Gadd and de Rome 1988). Melanin can function either intracellularly or extracellularly as a barrier against metal toxicity (Hong and Simon 2007; Cordero and Casadevall 2017) additionally a melanin molecule is capable of chelating multiple metal ions (Hong and Simon 2007). Melanin has a high affinity for heavy metal ions such as lead, iron, and copper (Gadd and de Rome 1988) the latter two being of specific biological significance due their role in oxidative stress (Gadd 1984; Gadd and de Rome 1988, Cervantes and Gutierrez-Corona 1994), further supporting its role as multifaceted protective agent. This property of melanin in fungi presents many opportunities in bioelectronic materials as the chelating capabilities of melanin could allow it to function as a mediator between inorganic and organic molecules (Di Mauro et al. 2017), to say nothing of the mentioned inherent conductive properties as well.

1.2 Objectives

Given the unique conductive properties of melanin, there are many potential electronics applications as it could serve as an organic charge carrier. We further theorized that given these same properties and the presence of melanin within the cell walls of fungi, it could also serve as a conduit for electrical signals while still part of the organism. Because melanin has also shown to be an efficient chelator of metal ions, we also theorized that when exposed to metal ions, the melanin would bind them and further improve the conductivity, similar to how doping (the intentional introduction of impurities) increases the conductivity of semiconductors by increasing the concentration of charge carriers (Jastrzebska et al. 1996). We hypothesized that if additional metal ions (specifically copper) were available for chelation, then the conductivity of melanin in a cellular context would increase to a level comparable to pure synthetic melanin. To address this hypothesis, we sought to accomplish the following objectives:

1. Identify a nonvirulent melanin-producing fungal candidate for study.
2. Compare the conductivity of melanized fungal cells to purified synthetic melanin.
3. Determine the tolerance of a fungal culture to copper so it could be effectively grown in its presence.
4. Evaluate how the addition of copper to fungal growth media affects the conductivity of the cells.

1.3 Approach

To study and evaluate the conductive properties of our fungal candidates, we combined culturing techniques with electrical engineering and materials testing. We cultured three fungal candidate species: *Kluyveromyces marxianus*, *Aureobasidium melanogenum,* and *Curvularia lunata*. Only candidates that produced melanin in the laboratory were evaluated for conductive properties. Further analysis consisted of measuring the conductivity of both the fungal biomass and synthetic melanin. To examine how metal ions affect conductivity, we added copper to the growth media. In so doing, we sought to reveal the intrinsic conductive nature of melanized biomass and the impact of copper doping and thus begin to understand how melanized fungi could function as a biological carrier of electrical signals.

2 Methods

2.1 Fungal candidate culturing

2.1.1 Fungal species selection

The American Type Culture Collection (Manassas, VA, USA) provided the following fungal species: *Kluyveromyces marxianus* (ATCC® 26548; Rech et al. 1999), *Aureobasidium pullulans* var. *(*ATCC® 15233*;* Hermanides-Nijhof 1977*), and Curvularia lunata* (ATCC® 42011; Malik et al. 1979). Criteria for species selection included no known virulence and documented production of melanin when grown under laboratory conditions (Hewedy and Ashour 2009; Siehr 1981; Rižner and Wheeler 2003).

2.1.2 Media preparation

To promote the growth of the fungal candidates, several types of broth and agar plates were created according to the nutrient and growth requirements of the fungi and the recommendations of the supplier.

Agar: All agar was prepared in accordance with standard preparation techniques. Ingredients were completely dissolved on a stirring hot plate and then autoclaved such that the liquid temperature reached 121°C and 6.9 kPa for at least 25 minutes. Molten agar was then allowed to cool slightly before being poured into sterile petri plates.

Broths: The ingredients were combined and dissolved before they were autoclaved, such that the liquid temperature reached 121°C and 6.9 kPa for at least 25 minutes.

Yeast malt agar/broth (*K. marxianus* and *A. pullulans*): Yeast malt broth (YMB) was made up with the following concentrations of ingredients in deionized water: 3.0 g/L yeast extract, 3.0 g/L malt extract, 10.0 g/L dextrose, and 5.0 g/L peptone. The recipe for yeast malt agar (YMA) was the same as for YMB but with the addition of 20.0 g/L agar.

Malt extract agar/broth and thickened malt extract broth (*C. lunata)*: Malt extract broth (MEB) was made up with the following concentrations of ingredients in deionized water: 20 g/L malt extract and 5 g/L peptone. Malt extract agar (MEA) contained the same ingredients as MEB

but with the addition of 20 g/L agar. To make thickened malt extract broth (tMEB), standard MEB was prepared with the addition of 2 g/L agar.

Yeast extract peptone D-xylose agar/broth (*K. marxianus* and *A. pullulans*): Yeast extract peptone D-xylose broth (YEPDxyl) was made by combining the following concentrations of ingredients in deionized water: 20 g/L D-xylose, 5 g/L yeast extract, 5 g/L peptone, and 5 g/L NaCl. YEPDxyl agar plates were made using the recipe of the YEPDxyl broth with the addition of 20 g/L agar.

Potato dextrose agar/broth and thickened potato dextrose broth (*C. lunata*): Potato Dextrose Broth (PDB) was made following the manufacturer's (BD, Franklin Lakes, NJ, USA) recommendation of 24 g/L potato dextrose broth powder in deionized water. Similarly, potato dextrose agar (PDA) was made under the manufacturer's (BD, Franklin Lakes, NJ, USA) instruction of 39 g/L potato dextrose agar powder in deionized water. Thickened potato dextrose broth (tPDB)was made by combining 2 g/L agar with standard PDB.

2.1.3 Propagation and culturing

Fungi were received in a dried state and revived following the manufacturer's instructions. Each dehydrated organism was rehydrated in 6 mL sterile filtered water and incubated at room temperature (approximately 23°C) for 24 hours prior to inoculation in the appropriate growth media.

The rehydrated fungal stocks were initially inoculated in various medias (broth and agar plates) as described below. The fungal candidates (500 µL) were inoculated in 30 mL of either YMB or MEB depending on the fungi's nutrient requirements. The inoculated cultures were mixed well and placed in an orbital shaking incubator set at 120 rotations per minute (RPMs) and 28°C.

YMA and MEA plates were inoculated by taking 200 µL of the rehydrated cultures, pipetting onto the plates, and spreading them on the appropriate plates using a flame-sterilized glass spreader. The inoculated plates were placed in an incubator set to 28°C. In both cases, uninoculated broth flasks and agar plates containing only media as a control were kept with the inoculated samples to check for contamination. The cultures were monitored for growth and production of dark pigmentation, suggesting the creation of melanin.

To improve or promote melanin production, the fungal candidates were also cultured in media demonstrated in the literature to elicit the generation of melanin. The 500 µL of the rehydrated spores for *K. marxianus* and *A. pullulans* were added to 30 mL of YEPDxyl. Then, 100 µL of the rehydrated cells were also spot plated on YEPDxyl agar plates. Both cultures were put into an incubator set to 32°C (Hewedy and Ashour 2009), the broth cultures were set on an orbital shaker set to 120 RPM, and the plates were put on a shelf. The organisms were monitored for 10 days.

The melanin-producing colonies of *C. lunata* were cultured on tMEB to allow for more stability and improved growth. Then, 500 µL of the previous melanin-producing *C. lunata* cultures grown in MEB were added to sterilized tMEB and incubated on an orbital shaker at 28°C. Additionally, *C. lunata* also propagated on tPDB and PDA. To inoculate the tPDB, 3 × 3 mm plugs of the melanin-producing *C. lunata* cultures grown on MEA were cut out using a flame-sterilized scalpel and transferred to 30 mL of sterilized tPDB in a 125 mL flask. PDA was inoculated by taking 3 × 3 mm plugs using a flame-sterilized scalpel of the same MEA cultures, dabbing them around the center of the PDA plate, and then depositing the plug in the center culture-side down. All inoculated tPDB and PDA plates were incubated at 28°C. All tPDB flasks were set on an orbital shaker within the incubator set at 120 RPM, and PDA plates were on a shelf in the same incubator.

2.2 Copper tolerance assay

To ascertain the concentration of copper sulfate *C. lunata* could tolerate without suffering deleterious effects in growth or appearance, we performed a copper tolerance assay. The 40 mM of copper sulfate stock was prepared by suspending copper sulfate in deionized water and then filter sterilizing (0.22 µm) the stock via vacuum filtration. Next, varying concentrations of copper sulfate agar plates of PDA were made by following the protocol for PDA described in section 2.1.2). Additionally, the sterilized molten PDA was transferred to five sterilized 250 mL Nalgene bottles. Each bottle corresponded to a concentration of copper sulfate (0.0 mM, 0.01 mM, 0.10 mM, 0.5 mM, and 1 mM) and was brought to that concentration by adding the appropriate amount of 40 mM copper sulfate to the PDA such that the final volume was 200 mL for each bottle. The copper-sulfate-containing molten agar was poured into sterile petri plates and allowed to cool.

To plate the organism, 2 × 2 mm fungal plugs of *C. lunata* were taken from the outer perimeter one of the PDA stock cultures with a flame-sterilized scalpel, dabbed gently on the surface of the plates containing copper sulfate, and then deposited culture side down on the center. Inoculated plates were incubated at 28°C for 10 days and then assessed for growth and tolerance.

2.3 Fungal biomass collection and preparation

Biomass was collected from mature cultures that had incubated for at least 10 days. To collect *C. lunata* biomass from agar media plates, cultures were scrapped off the agar surface using flame-sterilized scalpels and spatulas. Scrapped cultures from multiple plates were combined in one sterilized (autoclaved) glass petri plate until processing. The cultures were then put in a stainless-steel mesh filter and washed three times with boiling deionized water to remove any excess agar. Next, the cleaned felts were frozen for at least 2 hours in a −80°C freezer prior to being lyophilized on a VirTis FreezeMobile 12XL (Gardinar, NY, USA) overnight (12–16 hours).

Once samples were dried via lyophilizaton, they were milled using an Ika A11 Basic Analytical Mill (Wilmington, NC, USA) for 60 total seconds in 5 second pulses. Milled samples were stored in a desiccator until use.

2.4 Current-voltage sweeps

2.4.1 Scanning electron microscope material characterization

To visualize the materials and characterize their structure, high-resolution images of the synthetic melanin, fungal biomass, and copper-doped fungal biomass were captured with a scanning electron microscope (SEM) operating in a low-vacuum, backscatter imaging mode (Phenom ProX, Thermo Fisher Scientific, Waltham, MA, USA). The accelerating voltage was set to 10 kV. A small amount of melanin was sprinkled onto conductive carbon tape, which was attached to a standard SEM aluminum stub. Prior to loading the specimen into the SEM, excess melanin was removed with compressed air.

2.4.2 Pellet preparation

To provide samples of a consistent shape and a stable surface to attach electrodes to, each of our sample materials were pressed into circular pellets as in Mostert, Powel, Gentle, et al. (2012). Pellets were formed from

the milled biomass (copper doped and standard) and from commercial synthetic melanin (M8631, Sigma Millipore, Burlington, MA, USA) to function as a pure melanin comparison. The synthetic and milled samples were individually crushed using an agate mortar and pestle for 20 minutes to ensure reduction in particulate size and to improve pellet adhesion. Approximately 200 mg of powder was pressed into a 13 mm diameter pellet using a manual hydraulic pellet press (Specac Atlas 15T, Specac Ltd, Orpington, UK). The powder was loaded into the dye assembly, and the applied pressure was increased in increments of 1 ton every approximately 15 seconds and held at that pressure for 1 minute. The pressure was ultimately increased to 10 tons and held for 3 minutes. The resulting pellet appeared black and smooth with a somewhat shiny finish. If the pellet was of poor quality (i.e., with cracks or rough surface), it was ground up with the mortar and pestle, and the process was repeated. No vacuum was applied during the pellet-making process.

Platinum electrodes were deposited onto the freshly made pellet using a brass shadow mask. The electrode pattern was engraved onto the thin brass metal with a Printed Circuit Board engraver (ProtoMat S63, LPKF, Garbsen, Germany). Each square electrode area was ~5.67×10^{-2} cm^2, and the spacing between the four electrodes was ~1.587×10^{-1} cm. Platinum metal deposition was carried out for 60 seconds inside a sputtering chamber (Denton Vacuum DESK-II, Denton, Moorsetown, NJ, USA). To minimize motions due to vacuum pump vibrations, the pellet and the shadow mask were attached to the interior of the sputtering chamber with adhesive Scotch tape (3M, St. Paul, MN, USA). Immediately after the electrode deposition, the pellet was placed on a Teflon holder, and thin magnet wires (36 AWG) were attached to the electrodes with conductive silver paste (735825-25G, Sigma Aldrich; Burlington, MA, USA). The magnet wires were attached to the Teflon surface with Kapton tape (7770807, Fisher Scientific; Waltham, MA, USA).

2.4.3 Current-voltage characteristics

To obtain current-voltage characteristics, commonly used to determine how a material behaves under certain electrical impulses (e.g., current or voltage application), we performed current sweeps and measured the corresponding voltage. Sweeps were performed on the pellets of synthetic melanin (to serve as a baseline comparison), the copperless *C. lunata* biomass, and copper-doped *C. lunata* biomass. To minimize the effects of humidity, the pellet with the attached wires was stored inside a desiccator

jar. Measurements were carried out in the van der Pauw configurations (van der Pauw 1958) using a Keithley 2450 source meter unit. The source meter unit was programmed to provide a triangular current waveform while measuring voltage. A typical current sweep started from −2.5 nA, ramped up to 2.5 nA, and then ramped back down to −2.5 nA. The amplitude of the current sweep was chosen such that the measured voltage was within the limit of the SMU (20 V maximum). Eight configurations were tested for each pellet (Figure 4). Measurements were carried out in ambient environment (~50% relative humidity) at approximately 12 hours after attachment of the wires to the electrodes to ensure the silver paste had dried. As the synthetic melanin served as the baseline, replicate trials were conducted in triplicate whereas duplicate trials were conducted on the pelletized biomass.

The current-voltage curves were plotted within ggplot in R, and scatter plots of voltage versus current were smoothed using the Lowess method to aid in trend and pattern visualization (Wickham 2016; R Core Team 2013). To calculate the conductivity, the slope of the voltage versus current measurements was calculated using the linear regression model function within R.

Figure 4. Eight different positions of the van der Pauw configuration measurements. *I* represents current, and *V* represents voltage.

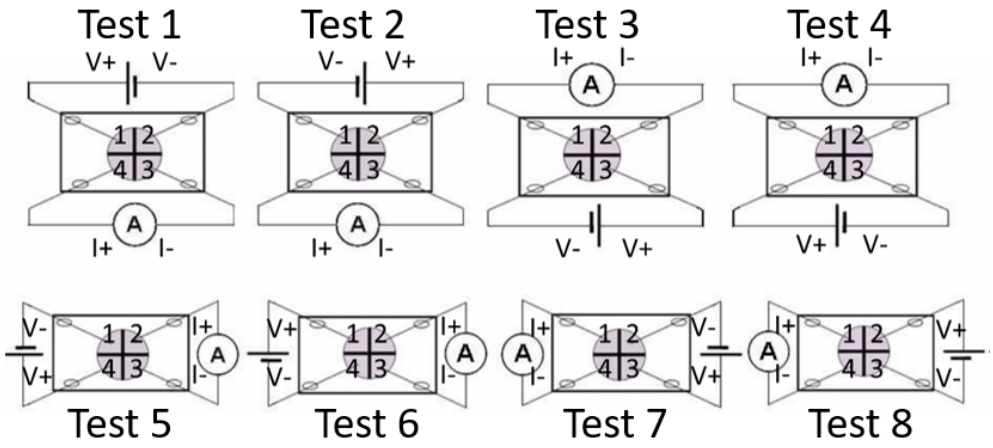

3 Results

3.1 Fungal candidate culturing

The first objective in this project was to determine if any of the fungal candidates selected could produce melanin in visible quantities. We initially cultured the three candidates cultured according to the manufactures' recommendations for media and incubation temperature to ensure proper revival and to ascertain regular growth. Then, in an attempt to optimize or initiate melanin production the media, we modified the culturing conditions to match parameters found in studies where melanin production was observed for the species in question.

3.1.1 Qualitative assessment of melanin production

All fungal cultures grown using the supplier's recommended agar and broth media (YMB and YMA: *K. marxianus* and *A. pullulans*) produced visible cultures within 1 to 2 days after inoculation. *K. marxianus* and *A. pullulans* appeared to be nonfilamentous in their growth as evidenced by the cloudy particulate appearance of the broth (Figure 5*A* and *B*) and slime-like appearance on the plates (Figure 6*A* and *B*). After 7 days, the *K. marxianus* and *A. pullulans* cultures had visible growth but little evidence of melanin production. The YEPDxyl media was selected for *K. marxianus* and *A. pullulans* to encourage the production of melanin as recommended in Hewedy and Ashour (2009). Xylose and peptone in the media have been shown to promote melanin production (Hewedy and Ashour 2009; Pradeep and Pradeep 2013; El-Naggar and El-Ewasy 2017). After incubating for 10 days, melanin production was not observed in *K. marxianus* and *A. pullulans* (Figure 7*A* and *B*); therefore, this study did not use them further.

Curvularia lunata was grown initially using the supplier's recommended plate and broth media (MEB). *C. lunata* appeared black and was a promising candidate for melanin production. *C. lunata* appeared filamentous when grown on solid media (Figure 6C) and grew as large hyphal aggregates in the initial broth (Figure 5C). At first we thought the agar cultures of *C. lunata* were be contaminated, as the first inoculated cultures appeared to have two species, one light and one dark (Figure 6C). However, we determined that the lighter culture was a different sexual state of *C. lunata* by comparing more mature cultures (greater than 20 days) to the

light culture (see Alex et al. 2013). Only the dark cultures were propagated for further analysis because of their potential melanin production.

Figure 5. Liquid cultures of (A) *Kluyveromyces marxianus*, (*B*) *Aureobasidium pullulans*, and (*C*) *Curvularia lunata* in YMB (*A*, *B*) and MEB (*C*).

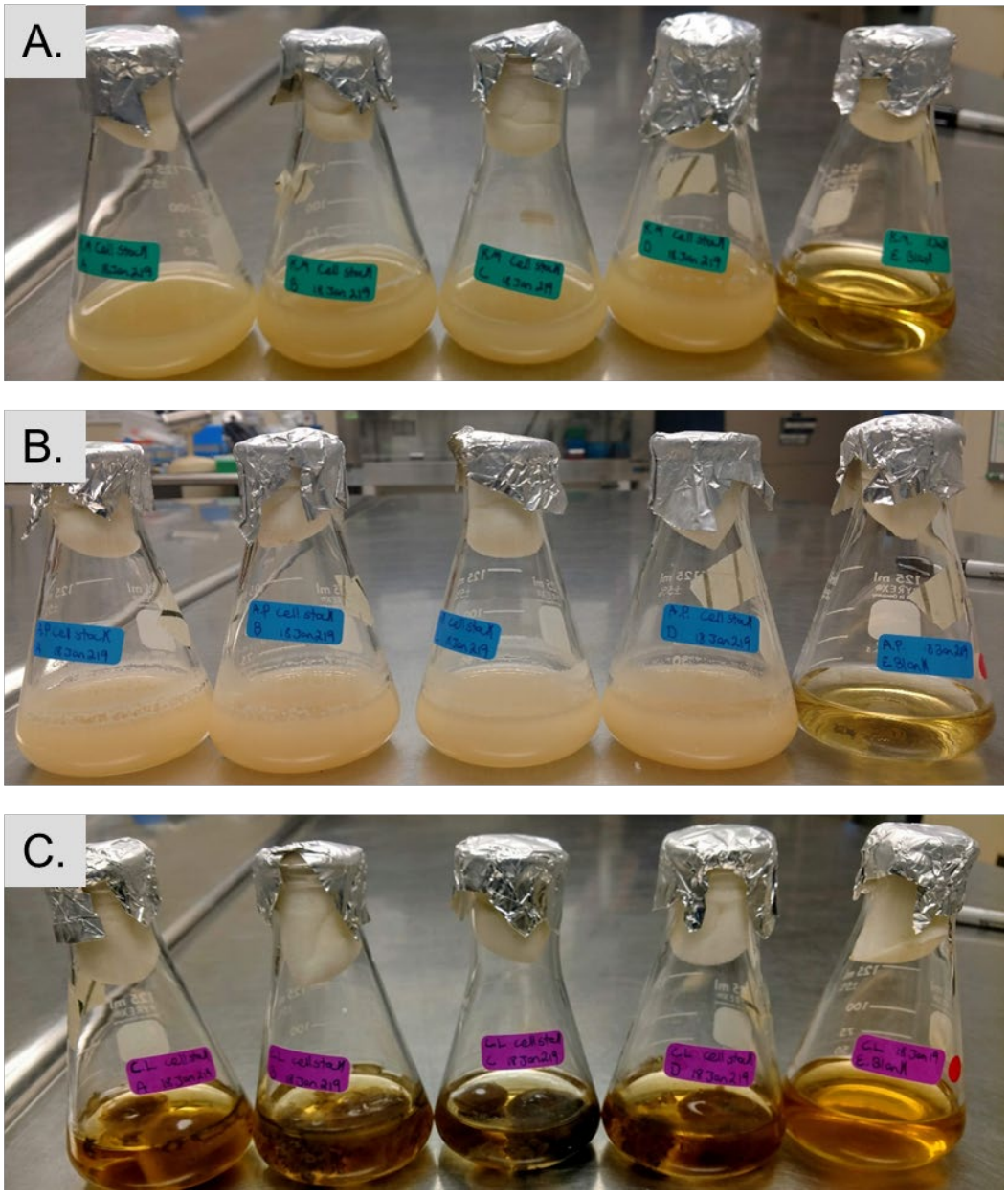

Figure 6. Plate cultures of (A) *Kluyveromyces marxianus* and (B) *Aureobasidium pullulans* grown on YMA and (C) *Curvularia lunata* grown on MEA.

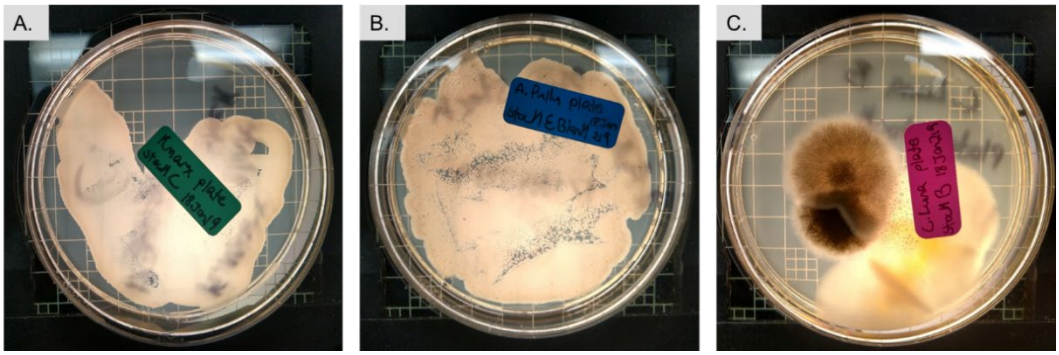

Figure 7. Liquid cultures of (A) *Kluyveromyces marxianus* and (B) *Aureobasidium pullulans* in YEPDxyl.

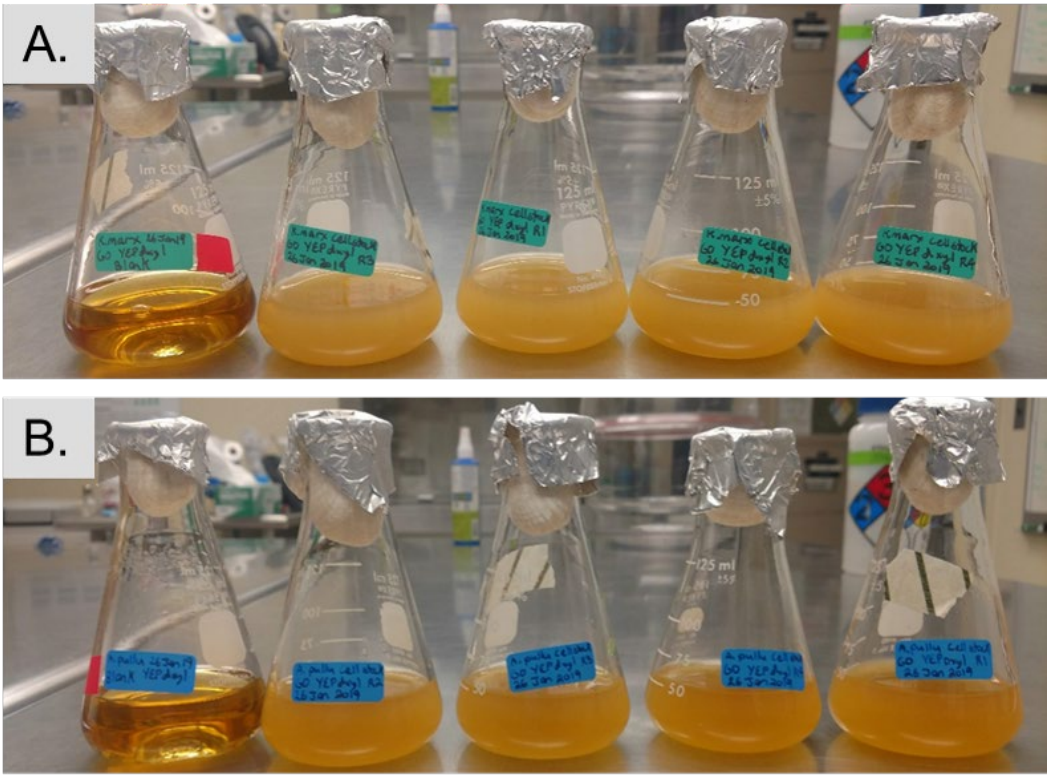

The aggregate-like growth of *C. lunata* was deemed suboptimal for potential melanin production as the hyphal aggregates were limited in size and only lightly pigmented. Therefore, the broth was thickened with agar (final concentration 2%) to provide more stability for growth by providing anchor points and to encourage mat formation. Additionally, to encourage melanin production, the growth media was altered to tMEB as the peptone, coenzymes, and vitamins in the media have been demonstrated to stimulate melanin production (Pradeep and Pradeep 2013). The change in

thickness for the broth used in *C. lunata* resulted in large cultures of 1–3 individual colonies after 3–5 days of incubation. The colonies became darkly pigmented, suggesting melanin production (Figure 8).

Selvakumar et al. (2008) suggested that PDB and PDA could encourage melanin production in *C. lunata*, and thus we used agar plugs from tMEB grown cultures to inoculate PDB and PDA media as well. Cultures grown on PDB and PDA appeared much darker than those grown in tMEB and on MEA. The cultures grown in PDB and on PDA also produced pigments throughout the culture after 1 day of incubation and appeared to grow a thicker felt-like mat on the agar than cultures grown on MEA (Figure 9).

Figure 8. Replicate liquid cultures of *Curvularia lunata* in tMEB: (*A*) starting culture, (*B*) incubation after 10 days, and *red-labeled* flask is media control. Replicates show different levels of apparent melanin, ranging from dark brown to black.

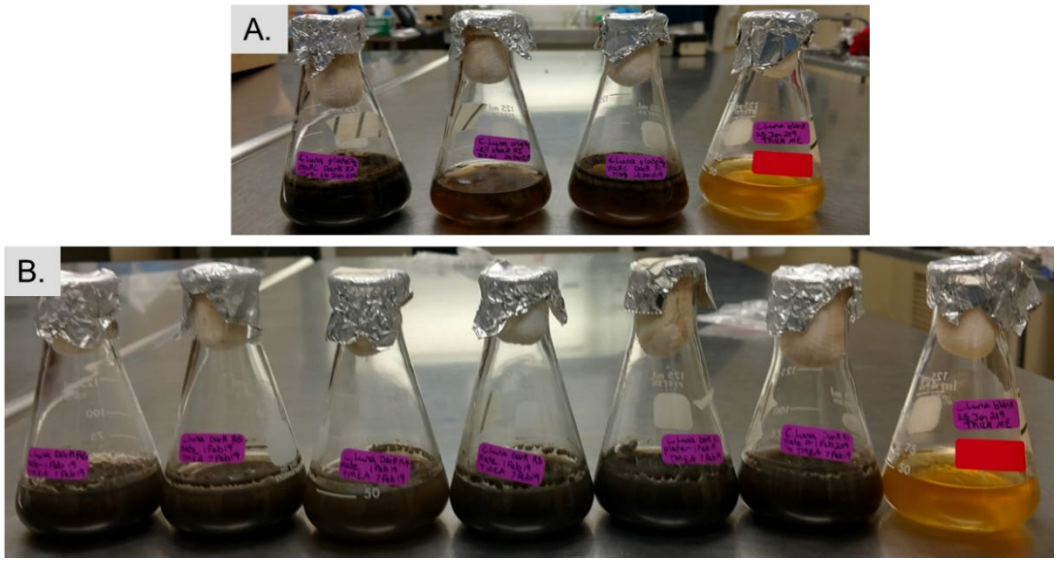

Figure 9. The 2-day (*A*) and 10-day (*B*) cultures of *Curvularia lunata* on potato dextrose agar.

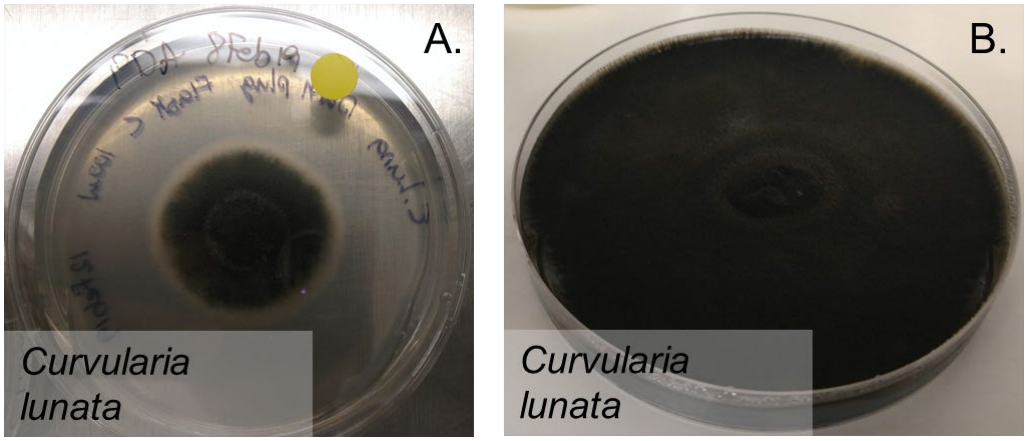

In the PDB, cultures produced large singular dark mats that consumed the entirety of the liquid present in the container into the cultures' biomass unlike the tMEB cultures, which produced a limited number of smaller individual colonies. As the cultures grown on PDA and PDB produced larger cultures with potentially more melanin, all further analyses used *C. lunata* cultures grown on PDA and PDB.

3.1.2 Copper tolerance assay

To determine a sublethal concentration of copper that would not harm the growth of the organism but would potentially allow for binding to the cellular melanin, we performed a growth phenotype assay. *C. lunata* was grown on PDA with no addition of copper sulfate and four increasing concentrations of copper sulfate: 0.01 mM, 0.10 mM, 0.50 mM, and 1.00 mM. Concentrations of 0.5 mM and 1.0 mM copper sulfate inhibited growth (Figure 10). Melanin production and fungal growth did not appear adversely affected by the addition of 0.01 mM or 0.1 mM copper sulfate (Figure 10). Therefore, further experimentation used PDA plates containing 0.1 mM copper sulfate.

Figure 10. Cultures of *Curvularia lunata* exposed to increasing concentrations of copper sulfate after 10 days. Rows represent replicate cultures.

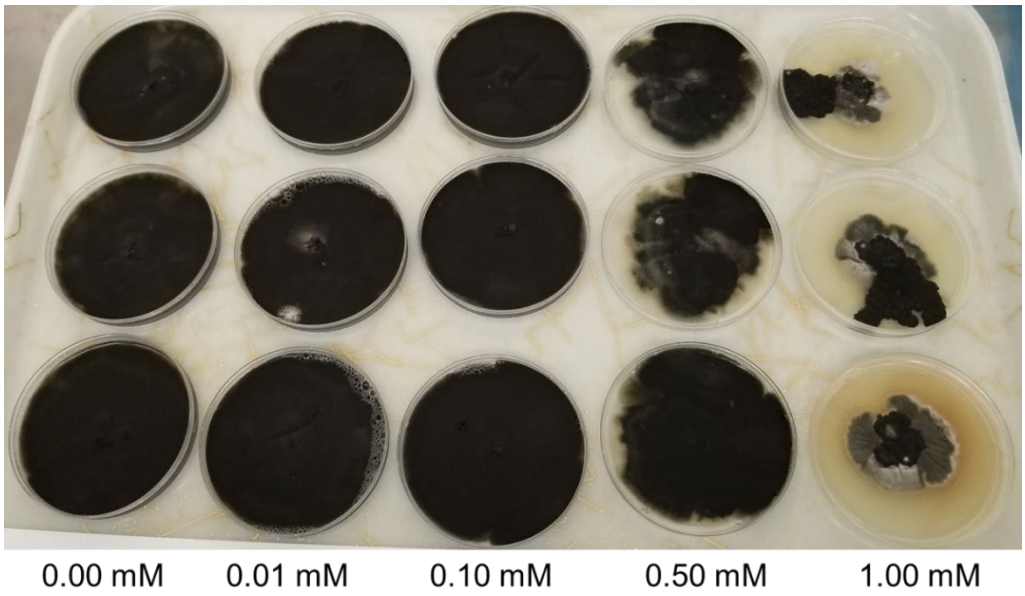

3.2 Scanning electron microscope imaging

To better understand and investigate structural properties of the materials used in this study, we imaged them with a scanning electron microscope.

3.2.1 Synthetic melanin

SEM scans of the synthetic melanin revealed the powder to have a fairly uniform granular structure (Figure 11). Individual granules of melanin ranged from less than 1 µm to approximately 3 µm in size.

Figure 11. Scanning electron microscope image of synthetic melanin.

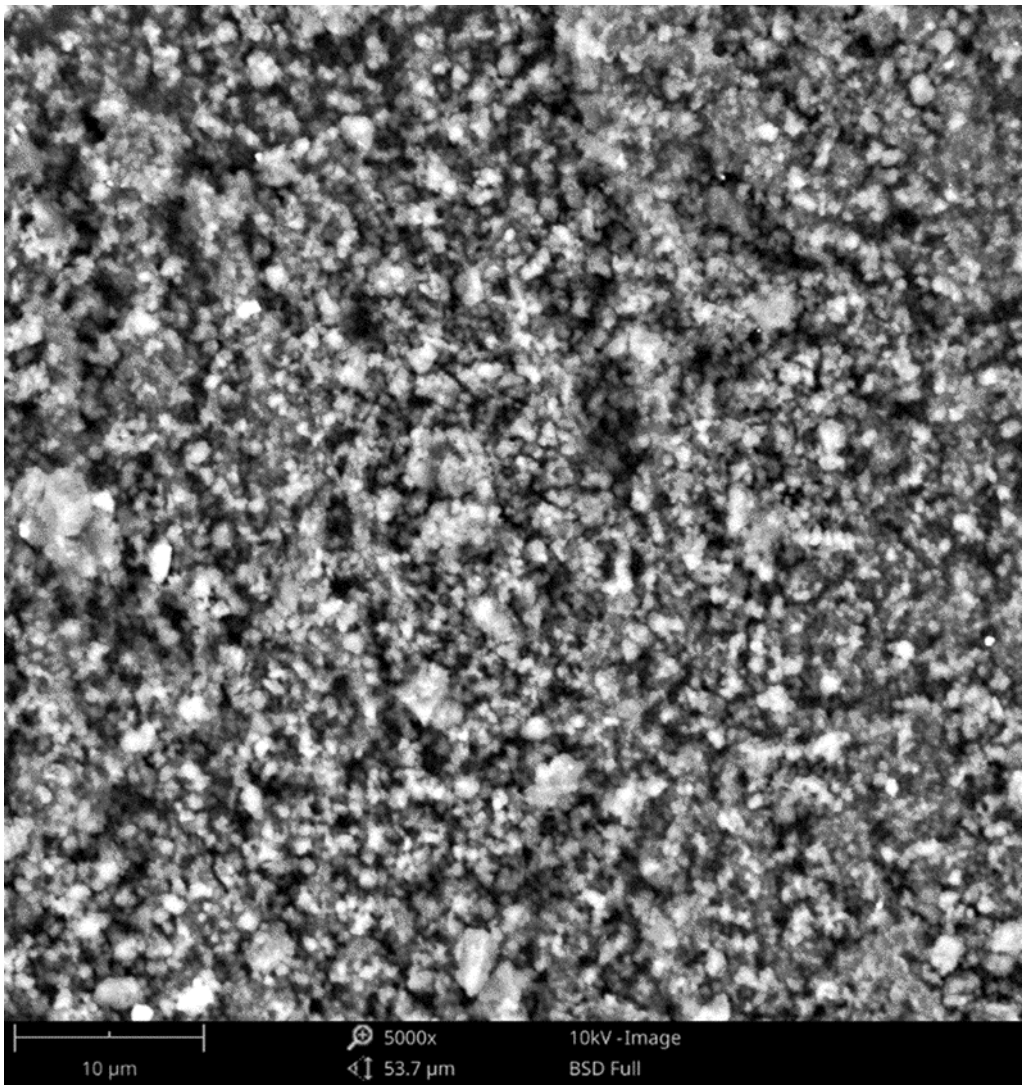

3.2.2 *C. lunata* biomass

Scans of the *C. lunata* biomass show that after milling the sample was composed of many types of fungal cells and structures both intact and partially intact. The long tube-like structures are likely conidiophores or hyphae, elongated stalk-like structures used to disperse conidia, the smaller raisin-like spores of *C. lunata* (Figure 12) (Babu et al. 2018).

Figure 12. Scanning electron microscope image of C. lunata biomass.

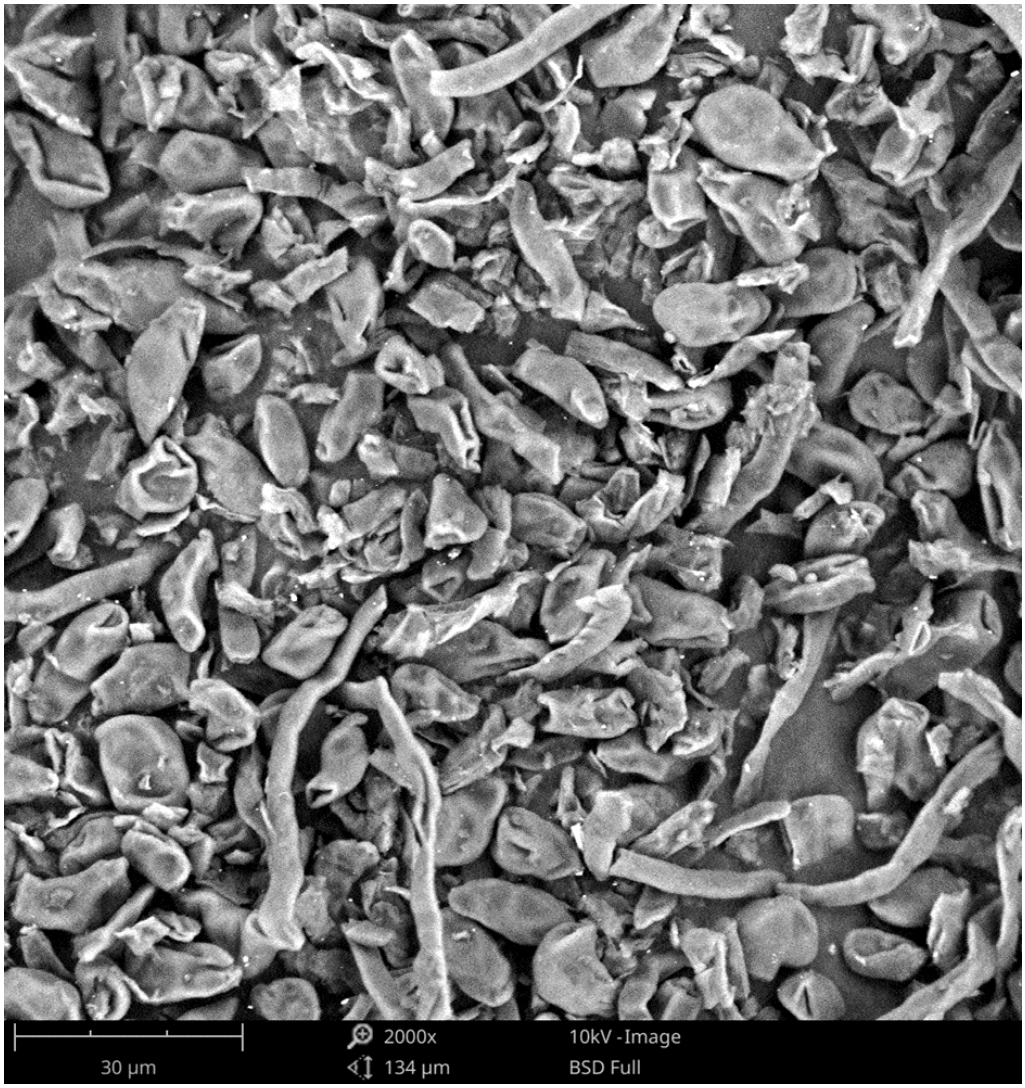

3.2.3 Copper-doped *C. lunata* biomass

Like the biomass produced in standard media, the copper-doped biomass was composed of many cells and structures of *C. lunata*. Both the conidia, conidiophores, and hyphae appeared to have both whole cells and fragments represented in the sample (Figure 13).

Figure 13. Scanning electron microscope of copper-doped C. lunata biomass.

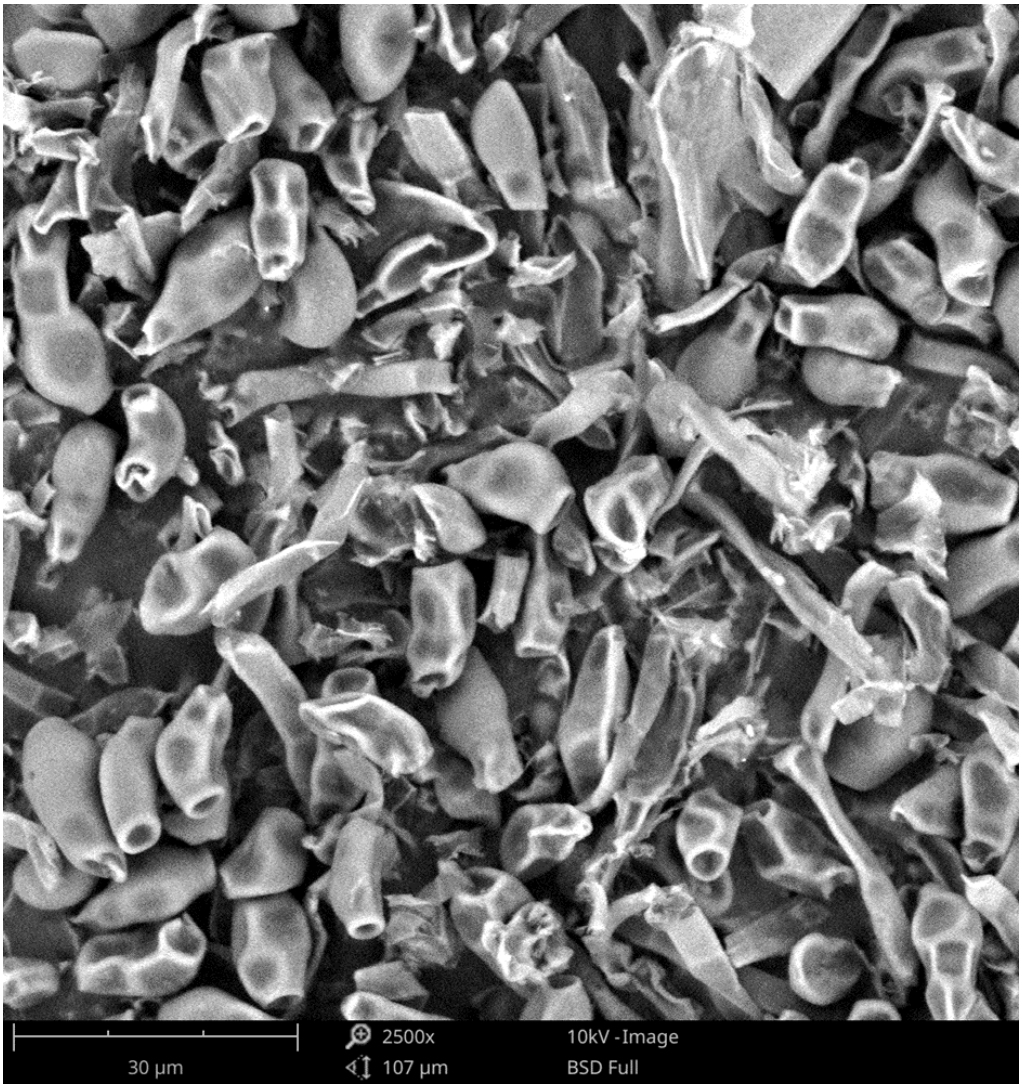

3.3 Current-voltage characteristics

3.3.1 Current-voltage characteristics of synthetic melanin

Synthetic melanin had a uniformly linear response (slope) to changes in current for all replicate measurements (Figure 14). While Figure 14 shows only test configuration 8, Appendix A shows all test configurations and replicates. The curve passes roughly through the origin and maintains a constant slope in all test configurations, both of which are behaviors observed in resistors. Current-voltage response was very similar across configurations (Figure A-1), suggesting relative spatial uniformity of the pelleted material.

Figure 14. Current-voltage characteristic curve of synthetic melanin pellets test configuration 8. Each point indicates one measurement event.

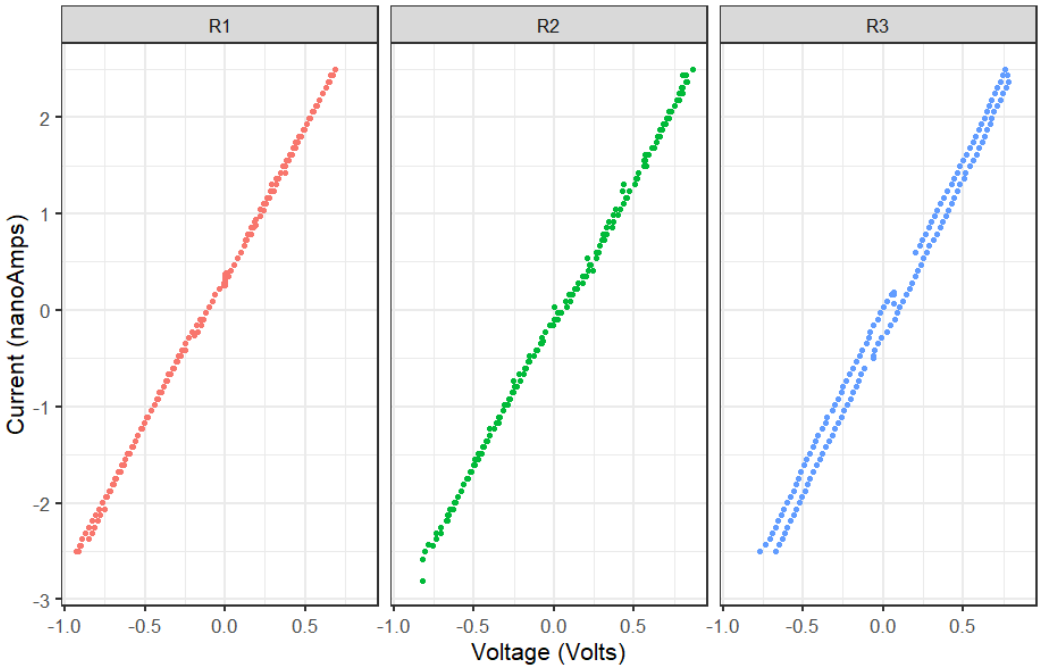

3.3.2 Current-voltage characteristics of *C. lunata* biomass

Pellets made of ground *C. lunata* biomass showed a heterogeneous response to applied current (Figure A-2). In configuration 8, when current increased, the measured voltage increased rapidly; the observed differences in voltage response across replicates (Figure 15) is likely due to electrochemical effects (Wunsche et al. 2015). The voltage response behaved linearly in isolated sections of middle to low current, which is also behavior observed in semiconductive material. The current-voltage relationship, however, varied substantially between replicate measurements (Figure 15). This variability could be attributed to both the surface heterogeneity of the pellet as demonstrated in the dissimilarity of curves between test configurations (Figure A-2). Test configurations 2, 3, 5, and 7 showed the greatest difference between replicates, though the reason why these configurations in particular are more variable is unclear (Figure A-2).

Figure 15. Current-voltage characteristic curves of copperless *C. Lunata* biomass test configuration 8. Each point indicates one measurement event.

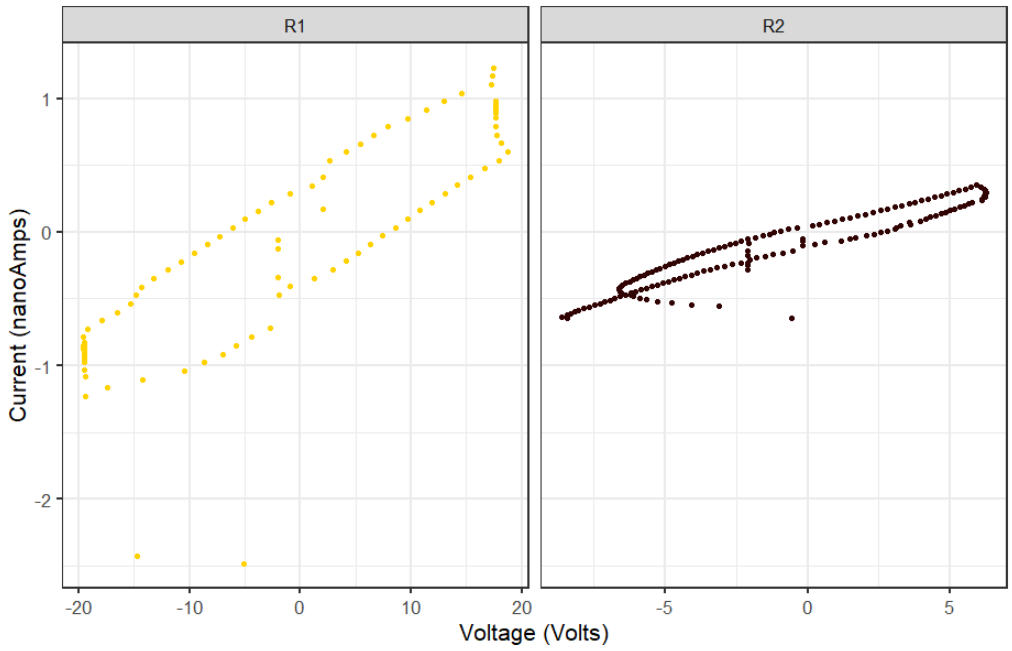

3.3.3 Current-voltage sweep of copper-doped *C. lunata*

Results from the copper-doped *C. lunata* pellets were highly variable across test configurations (Figure A-3), suggesting the heterogeneity of the pellet surface due to the irregularity of the material (i.e., microscale differences of cell abundance, shape, size, etc.) (Figure 16). Test configuration 8 shows the most linear response of the configurations in a similar form to the synthetic melanin. However, several configurations showed abnormalities. Test configuration 1 specifically demonstrated an erroneous current range in replicate 1 as it far exceeded the maximum values of all other tests (Figure A-3). Tests configurations 5 and 7 also demonstrated an abnormal voltage range in comparison to the other configurations and between the replicates (Figure A-3). Configurations 2, 3, 5, and 7 registered a very narrow range of voltages (−2.5 V to 2.5 V) which was lower than that of the other configurations, which ranged between −5 and 5 V (Figure A-3).

Figure 16. Current-voltage characteristic curves of copper-doped *C. lunata* biomass test configuration 8. Each point indicates one measurement event.

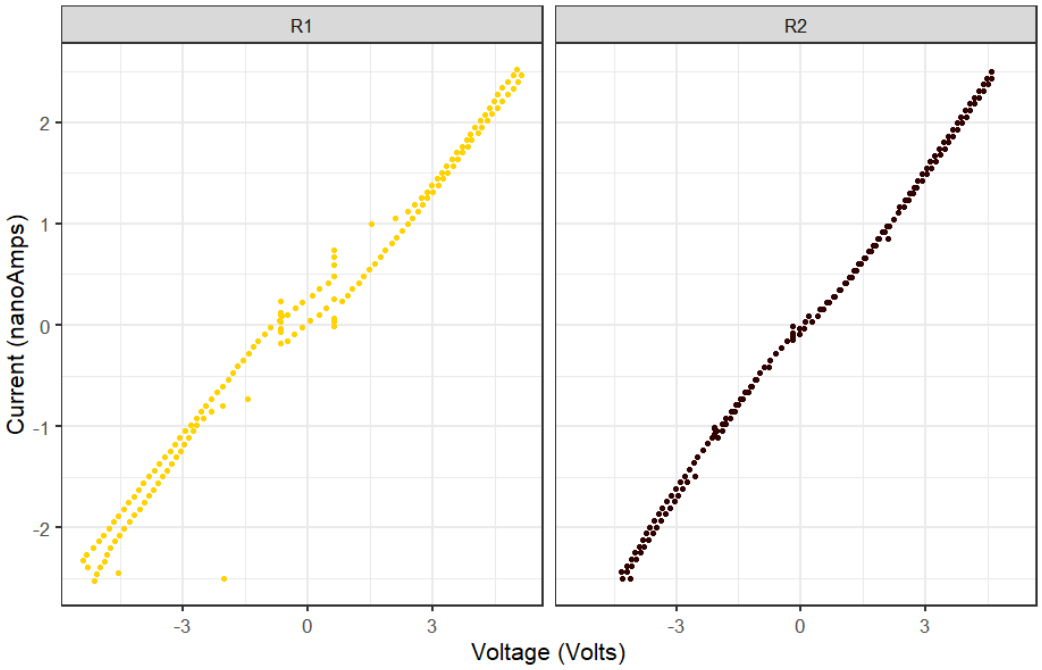

3.3.4 Comparison across all sample types

To compare the conductivity of the tested materials, the smoothed line averages of the test configurations in which all samples had a linear relationship between current and voltage were potted together (Figure 17). Synthetic melanin was the most conductive as it has a steeper slope than both the copper-doped and copperless *C. lunata* samples (Figure 17). The conductivity of synthetic melanin was at least an order of magnitude higher than either of the biologically derived samples (Table 1). The copper-doped *C. lunata* pellets, while less conductive than the synthetic melanin, had greater conductivity than the copperless *C. lunata* pellets by an order of magnitude. The *C. lunata* sample alone had a very shallow slope, indicative of a stronger insulative tendency and further supported by its low conductivity of 3.47×10^{-13} S/cm. This suggests that the presence of copper in the media improved the conductivity of pelleted *C. lunata* biomass.

Figure 17. Comparative current-voltage characteristic curves of synthetic melanin, copper-doped, and copperless *C. lunata* biomass.

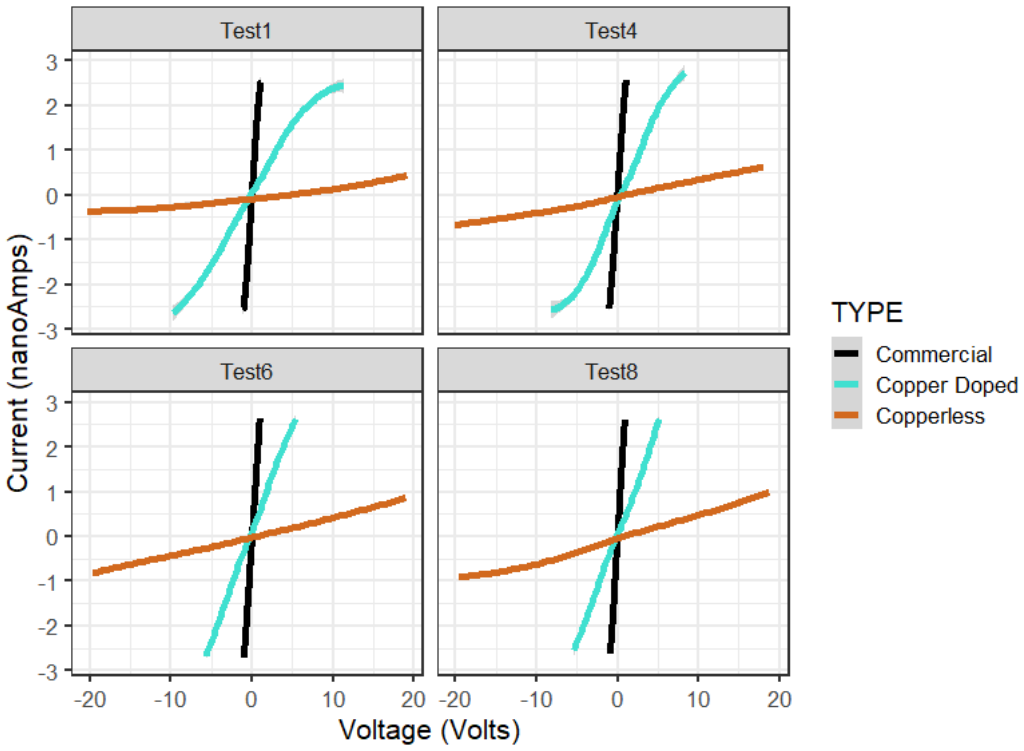

Table 1. Conductivity of synthetic, copper-doped, and copperless samples.

Sample Type	Conductivity σ (S/m)	Conductivity σ (S/cm)
Commercial Synthetic	2.759e-09	2.759e-11
Copper-doped	4.048e-10	4.048e-12
Copperless	3.470e-11	3.470e-13

4 Discussion

Synthetic and extracted melanins possess a wide array of properties, principally electrical conductivity and broad affinity for binding to molecules, such as heavy metals (Jastrzebska et al. 1996, 2002; Hong and Simon 2007; Mostert, Powell, Pratt, et al. 2012). There is, however, limited knowledge of the conductive properties of biological melanin while it is still bound to or in host cells and how molecules bound to melanin may influence the conductivity as they can change the balance of electron carriers (Hong and Simon 2007). Fungi are known producers of melanin, which can aggregate within the fungal cell wall. Fungi have also demonstrated the use of their melanin to bind toxic metals (Cu, Pb, Zn, etc.) from the environment to prevent damage to cellular components (Gadd and de Rome 1988; Fogarty et al. 1996), forming metal-melanin complexes, similar to material doping. By performing current-voltage sweeps on synthetic melanin, melanized *C. lunata* biomass, and melanized *C. lunata* biomass grown in copper-containing media, we were able to compare their electrical characteristics, such as conductivity. We demonstrated that while the melanized fungal biomass had lower conductivity than synthetic melanin, the presence of copper in the media may have influenced changes in the fungal biomass (either through binding or induced structural changes) to increase the conductivity.

The conductivity of synthetic melanin has been experimentally defined in a large range. Specifically, synthetically derived melanin has demonstrated conductivities ranging from the unprecedented high conductivity, 318 S/cm, demonstrated by Migliaccio et al. (2019) using vacuum-annealed melanin, to the more moderate measurements, 10^{-13} to 10^{-5} S/cm, demonstrated in one of the initial studies performed Jastrzebska et al. (1996) on chemically synthesized pelleted melanin. In our study, the conductivities measured from 10^{-13} to 10^{-11} S/cm, which fall within the range of the Jastrzebska (1996) study though are certainly on the more insulative end of the conductivity spectrum (i.e., higher resistance). However, this is a highly promising result as it demonstrates the potential to achieve comparable conductivity to synthetic melanin using melanized fungal biomass despite the melanin being bound in a fungal cell.

While there are many to variables to consider that could influence the conductivity of cellular melanin, the conductivity of pure melanin is still under

review. Many factors have been shown to impact synthetic melanin conductivity, such as hydration state, light, and temperature (Jastrzebska et al. 1996, 2002; Morresi et al. 2010), that future studies involving cellular melanin should consider. Temperature in particular can strongly influence melanin conductivity as Morresi et al. (2010) demonstrated, finding that between 300 K and 480 K, the conductivity of synthetic melanin increased from 10^{-13} S/cm to 10^{-6} S/cm, showing a broad sweep of temperature-dependent conductivity and again encapsulating the range of the conductivity observed in this study. In fact, until Migliaccio et al. (2019) achieved a conductivity of 318 S/cm, 10^{-5} S/cm was the highest conductivity reported for synthetic melanins, which would classify it as a moderately conductive material (Matijasevic and Brandt 2009). With Migliaccio et al. (2019) being a notable exception, manipulating melanin to achieve conductivity above 10^{-5} S/cm has been a challenging endeavor due in part to our incomplete understanding of the current generation and transport mechanisms for electrons (Meredith and Sarna 2006). While the impact of environmental factors on melanin have been studied, to our knowledge, though, there is limited research directly describing the impact that other biological molecules might have on the conductivity of melanin as would be relevant to this study.

Testing the conductivity of a biological material is challenging, as the material is often irregularly structured and can be strongly influenced by even minute changes in environmental factors, such as temperature and humidity (Meredith and Sarna 2006). In the case of the melanized fungal biomass, it is likely that the heterogeneous nature of the material (Figures 12 and 13) used in the sample pellet caused surface irregularities that influenced how current passed through the sample. Unlike the synthetic melanin, which was fairly uniform, the microstructures created when pelletizing the fungal biomass likely formed complex pathways for current to travel that invariably limited the viable configurations, as evidenced by the observed differences in the current-voltage curves. This highlights the importance of material uniformity in conductivity and perhaps the limitations of biological material to meet that level of uniformity. It is possible that were the fungal biomass to be ordered or structured more consistently, the conductive properties would improve. As several studies have shown, how melanin is structured and dispersed can impact the overall conductivity (Bothma et al. 2008, Bernsmann et al. 2009). Thin sheets having shown a higher conductivity than unstructured melanin (Morresi et al. 2010). This is further supported by Migliaccio et al. (2019), which

demonstrated that the melanin sheets that formed through the vacuum-annealing process played an integral role in improving the conductivity of melanin, and it is possible that this structural advantage could be mirrored in the orientation of the material or how melanin is organized within the cell wall. However, this cannot account for the other inhibitors present in samples. For future research, we would carry out specimen fabrication and electrical measurements in environmentally controlled conditions (i.e., inside and in an environmental chamber) to limit the influence of environmental conditions. Further, testing melanin films instead of pellets could yield samples with improved electrical performance. This is because films, when created under optimized fabrication conditions, generally have more-controlled morphology and fewer defects than bulk pellets. Finally, use of clean-room, lithographic techniques to deposit high-quality electrodes on the melanin surfaces would likely be beneficial in future experiments. Lithography ensures high-fidelity patterning and miniaturization of electrodes, compatible with existing device technologies.

We used melanized fungal biomass as a first step in understanding the electrical characteristics, particularly conductivity, of more intact and continuous melanized fungal structures such as a melanized mycelium. However, this included additional biomolecules (proteins, lipid layers, chitin, etc.) for the current to interact with, which could inhibit the electron flow. This, in addition to the aforementioned surface heterogeneity, are possible explanations for why the synthetic melanin was more conductive than the melanized fungal biomass even with the addition of copper ions. It is also worth noting that in the preparation of the pellet in our study, the fungal biomass samples were freeze dried, and thus the amount of available water was highly reduced. It is possible that fully hydrated melanized fungal biomass could have improved conductance as hydration state has been shown to be an integral aspect of melanin conductivity (Jastrzebska et al. 1996). More research is necessary that investigates how concentration and type of ion contributes to this effect and the impacts of the hydration state, but this study serves as preliminary data demonstrating the potential of metal ions to increase the conductivity of fungal biomass.

Additionally, while we found that the fungal biomass is more conductive when grown in the presence of copper, this does not prove that copper was actively chelated to the melanin within the biomass. To ascertain whether the increase in conductivity is from the binding of copper to melanin molecules (the doping effect) will require further research, such as identifying

characteristic structural changes via infrared spectroscopy (Bilińska et al. 2001). However, recent research focusing on electrolytic conductivity demonstrated that the conductivity of plant-derived melanin was greatly improved after the melanin molecules had bound to metal ions (Madkhali et al. 2019). Our research suggests that there is potential for a similar effect to occur in intracellular melanin.

5 Conclusion

Our objective was to assess the conductive characteristics of melanized fungal biomasses from our melanin-producing fungal candidate cultures compared to synthetic melanin and to examine how the presence of metal ions in the growth media might influence the conductivity. Our results demonstrated that relative to synthetic melanin, fungal biomass is less conductive. However, our results also suggest that when our candidate fungus, *Curvularia lunata*, is grown in copper-containing media, the biomass collected is more conductive in comparison to biomass produced on standard media. In spite of the improvement in the conductivity of the melanized fungal biomass, the tests indicate that on average the copper-doped biomass is less conductive than synthetic melanin. Numerous competing factors could cause this disparity, such as the comparative quantities of melanin, but it is likely primarily due to a combination of the irregular pellet structure and interference by other biological molecules.

Though synthetic melanin was several orders of magnitude more conductive than the melanized fungal biomass, our results suggest that the conductive properties of the biomass can be modified through fairly simple means, such as growing the fungi in the presence of copper to increase conductivity. The limits of this improvement, such as the upper bounds of conductivity, will require further study that focuses on the fungal structures; orientation of melanin; and the type, concentration, and binding of conductive ions to the melanin. While our results found that the conductivity of melanized fungal biomass of our fungal candidate was not on par with synthetic melanin, we have demonstrated the potential for metal ions to influence the conductivity of melanized fungal biomass, which presents an exciting new avenue of exploration into fungal melanin and suggests that melanin can be conductive while bound to the cell wall. Given the potential for cellular melanin to be conductive, there are promising applications for fungally derived biobased electronics and the development of conductive fungal structures, such as wire connections.

References

Alex, D., D. Li, R. Calderone, and S. M. Peters. 2013. "Identification of *Curvularia lunata* by Polymerase Chain Reaction in a Case of Fungal Endophthalmitis." *Medical Mycology Case Reports* 2:137–140.

Ambrico, M., P. F. Ambrico, T. Ligonzo, A. Cardone, S. R. Cicco, M. d'Ischia, and G. M. Farinola. 2015. "From Commercial Tyrosine Polymers to a Tailored Polydopamine Platform: Concepts, Issues and Challenges En Route to Melanin-Based Bioelectronics." *Journal of Materials Chemistry C* 3 (25): 6413–6423.

Ashkenasy, N., W. S. Horne, and M. R. Ghadiri. 2006. "Design of Self-Assembling Peptide Nanotubes with Delocalized Electronic States." *Small* 2 (1): 99–102.

Babu, G. V., P. Perumal, S. Muthu, S. Pichai, K. S. Narayan, and S. Malairaj. 2018. "Enhanced Method for High Spatial Resolution Surface Imaging and Analysis of Fungal Spores using Scanning Electron Microscopy." *Scientific Reports* 8 (1): 1–10.

Barra, M., I. Bonadies, C. Carfagna, A. Cassinese, F. Cimino, O. Crescenzi, V. Criscuol, M. d'Ischia, M. G. Maglione, P. Manini, L. Migliaccio, A. Musto, A. Napolitano, A. Navarra, L. Panzella, S. Parisi, A. Pezzella, C. T. Prontera, and P. Tassini. 2016. "Eumelanin-Based Organic Bioelectronics: Myth or Reality? *MRS Advances* 1 (57): 3801–3810.

Bell, A. A., and N. H. Wheeler. 1986. "Biosynthesis and Functions of Fungal Melanins." *Annual Review of Phytopathology* 24:411–451.

Bernsmann, F., A. Ponche, C. Ringwald, J. Hemmerle, J. Raya, B. Bechinger, J. C. Voegel, P. Schaaf, and V. Ball. 2009. "Characterization of Dopamine–Melanin Growth on Silicon Oxide." *The Journal of Physical Chemistry C* 113 (19): 8234–8242.

Bilińska, B., 2001. "On the Structure of Human Hair Melanins from an Infrared Spectroscopy Analysis of Their Interactions with Cu2+ Ions." *Spectrochimica Acta Part A: Molecular and Biomolecular Spectroscopy* 57 (12): 2525–2533.

Bothma, J. P., J. De Boor, U. Divakar, P. E. Schwenn, and P. Meredith. 2008. "Device-Quality Electrically Conducting Melanin Thin Films." *Advanced Materials* 20 (18): 3539–3542.

Bruenger, F. W., B. J. Stover, and D. R. Atherton. 1967. "The Incorporation of Various Metal Ions into In Vivo- and In Vitro-Produced Melanin." *Radiation Research* 32 (1): 1–12.

Butler, M. J., R. B. Gardiner, and A. W. Day. 2009. "Melanin Synthesis by *Sclerotinia sclerotiorum*." *Mycologia* 101 (3): 296–304.

Camacho, E., R. Vij, C. Chrissian, R. Prados-Rosales, D. Gil, R. N. O'Meally, R. J. Cordero, R. N. Cole, J. M. McCaffery, R. E. Stark, and A. Casadevall. 2019. "The Structural Unit of Melanin in the Cell Wall of the Fungal Pathogen *Cryptococcus neoformans*." *Journal of Biological Chemistry* 294 (27): 10471–10489.

Capozzi, V. I. T. O., G. Perna, P. Carmone, A. Gallone, M. Lastella, E. Mezzenga, G. Quartucci, M. Ambrico, V. Augelli, P. F. Biagi, and T. Ligonzo. 2006. "Optical and Photoelectronic Properties of Melanin." *Thin Solid Films* 511:362–366.

Casadevall, A., A. Nakouzi, P. R. Crippa, and M. Eisner. 2012. "Fungal Melanins Differ in Planar Stacking Distances." *PLoS One* 7(2): e30299.

Casadevall, A., A. L. Rosas, and J. D. Nosanchuk. 2000. "Melanin and Virulence in *Cryptococcus neoformans*." *Current Opinion in Microbiology* 3 (4): 354–358.

Cervantes, C., and F. Gutierrez-Corona. 1994. "Copper Resistance Mechanisms in Bacteria and Fungi." *FEMS Microbiology Reviews* 14 (2): 121–137.

Cordero, R. J., and A. Casadevall. 2017. "Functions of Fungal Melanin beyond Virulence. Fungal Biology Reviews 31 (2): 99–112.

Dadachova, E., R. A. Bryan, X. Huang, T. Moadel, A. D. Schweitzer, P. Aisen, J. D. Nosanchuk, and A. Casadevall. 2007. "Ionizing Radiation Changes the Electronic Properties of Melanin and Enhances the Growth of Melanized Fungi." *PLoS ONE* 2 (5): e457. https://doi.org/10.1371/journal.pone.0000457.

Dadachova, E., and A. Casadevall. 2008. "Ionizing Radiation: How Fungi Cope, Adapt, and Exploit with the Help of Melanin." *Current Opinion in Microbiology* 11 (6): 525–531.

Di Mauro, E., R. Xu, G. Soliveri, and C. Santato. 2017. "Natural Melanin Pigments and Their Interfaces with Metal Ions and Oxides: Emerging Concepts and Technologies." *MRS Communications* 7 (2): 141–151.

d'Ischia, M., K. Wakamatsu, A. Napolitano, S. Briganti, J. C. Garcia-Borron, D. Kovacs, P. Meredith, A. Pezzella, M. Picardo, T. Sarna, and J. D. Simon. 2013. "Melanins and Melanogenesis: Methods, Standards, Protocols." *Pigment Cell & Melanoma Research* 26 (5): 616–633.

Eisenman, H. C., and A. Casadevall. 2012. "Synthesis and Assembly of Fungal Melanin." *Applied Microbiology and Biotechnology* 93 (3): 931–940.

El-Naggar, N. E.-A., and S. M. El-Ewasy. 2017. "Bioproduction, Characterization, Anticancer and Antioxidant Activities of Extracellular Melanin Pigment Produced by Newly Isolated Microbial Cell Factories *Streptomyces glaucescens* NEAE-H." *Scientific Reports* 7:42129.

Felix, C. C., J. S. Hyde, T. Sarna, and R. C. Sealy. 1978. "Interactions of Melanin with Metal Ions. Electron Spin Resonance Evidence for Chelate Complexes of Metal Ions with Free Radicals." *Journal of the American Chemical Society* 100 (12): 3922–3926.

Fink, H. W., and C. Schonenberger. 1999. "Electrical Conduction through DNA Molecules." *Nature* 398:407–410.

Fogarty, R. V., and J. M. Tobin. 1996. "Fungal Melanins and Their Interactions with Metals." *Enzyme and Microbial Technology* 19 (4):311–317.

Gadd, G. M. 1984. "Effect of Copper on *Auerobasidium pullulans* in Solid Medium: Adaptation Not Necessary for Tolerant Behaviour." *Transactions of the British Mycological Society* 82:546–549.

Gadd, G. M., and L. de Rome. 1988. "Biosorption of Copper by Fungal Melanin." *Environmental Microbiology* 29:610–617.

Graham, D. G. 1979. "On the Origin and Significance of Neuromelanin." *Archives of Pathology & Laboratory Medicine* 103 (7): 359–362.

Haining, R. L., and C. Achat-Mendes. 2017. "Neuromelanin, One of the Most Overlooked Molecules in Modern Medicine, Is Not a Spectator." *Neural Regeneration Research* 12 (3): 372–375.

Heinekamp, T., A. Thywissen, J. Macheleidt, S. Keller, V. Valiante, and A. Brakhage. 2013. *Aspergillus fumigatus* Melanins: Interference with the Host Endocytosis Pathway and Impact on Virulence. *Frontiers of Microbiology* 3:440.

Hermanides-Nijhof, E. J. 1977. "*Aureobasidium* and Allied Genera." *Studies in Mycology* 15:141–177.

Hewedy, M. A., and S. M. Ashour. 2009. "Production of a Melanin like Pigment by *Kluyveromyces marxianus* and *Streptomyces chibaensis*." *Australian Journal of Basic and Applied Sciences* 3 (2): 920–927.

Hong, L., and J. D. Simon. 2007."Current Understanding of the Binding Sites, Capacity, Affinity, and Biological Significance of Metals in Melanin." *The Journal of Physical Chemistry B* 111 (28): 7938–7947.

Ing, N. L., R. K. Spencer, S. H. Luong, H. D. Nguyen, and A. I. Hochbaum. 2018. "Electronic Conductivity in Biomimetic α-Helical Peptide Nanofibers and Gels." *ACS Nano* 12 (3): 2652–2661.

Ito, S., and K. Wakamatsu. 2008. "Chemistry of Mixed Melanogenesis—Pivotal Roles of Dopaquinone. Photochemistry and Photobiology." 84 (3): 582–592.

Jastrzebska, M. M., H. Isotalo, J. Paloheimo, and H. Stubb. 1996. "Electrical Conductivity of Synthetic DOPA-Melanin Polymer for Different Hydration States and Temperatures." *Journal of Biomaterials Science, Polymer Edition* 7 (7): 577–586. https://doi.org/10.1163/156856295X00490.

Jastrzebska, M. M., S. Jussila, and H. Isotalo. 1998. "Dielectric Response and ac Conductivity of Synthetic Dopa-Melanin Polymer." *Journal of Materials Science* 33 (16): 4023–4028.

Jastrzebska, M., A. Kocot, and L. Tajber. 2002. "Photoconductivity of Synthetic Dopa–Melanin Polymer." *Journal of Photochemistry and Photobiology B: Biology* 66 (3): 201–206.

Jeffery, G., K. Darling, and A. Whitmore, A., 1994. "Melanin and the Regulation of Mammalian Photoreceptor Topography." *European Journal of Neuroscience* 6 (4): 657–667. https://doi.org/10.1111/j.1460-9568.1994.tb00311.x.

Kumar, P., E. Di Mauro, S. Zhang, A. Pezzella, F. Soavi, C. Santato, and F. Cicoira. 2016. "Melanin-Based Flexible Supercapacitors." *Journal of Materials Chemistry C* 4 (40): 9516–9525.

Kunwar, A., B. Adhikary, S. Jayakumar, A. Barik, S. Chattopadhyay, S. Raghukumar, and K. I. Priyadarsini. 2012. "Melanin, a Promising Radioprotector: Mechanisms of Actions in a Mice Model." *Toxicology and Applied Pharmacology* 264 (2): 202–211.

Langfelder, K., M. Streibel, B. Jahn, G. Haase, and A. A. Brakhage. 2003. "Biosynthesis of Fungal Melanins and their Importance for Human Pathogenic Fungi." *Fungal Genetics and Biology* 38 (2): 143–158.

Lovley, D. R., and D. J. F. Walker. 2019. "Geobacter Protein Nanowires." *Frontiers of Microbiology* 10:2078.

Madkhali, N., H. R. Alqahtani, S. Al-Terary, A. Laref, and A. Haseeb. 2019. "The Doping Effect of Fe, Cu and Zn Ions on the Structural and Electrochemical Properties and the Thermostability of Natural Melanin Extracted from *Nigella sativa* L." *Journal of Molecular Liquids* 285:436–443. https://doi.org/10.1016/j.molliq.2019.04.063.

Malik. K. A., N. A. Bhatti, and F. Kauser. 1979. "Effect of Soil Salinity on Decomposition and Humification of Organic Matter by Some Cellulolytic Fungi." *Mycologia* 71:811–820. https://doi.org/10.1080/00275514.1979.12021074.

Matijasevic, G., and L. Brandt. 2009. "Conductive Materials, Wires, and Cables." *Electrical Engineering* 2: 17–40.

McGinness, J., P. Corry, and P. Proctor. 1974. "Amorphous Semiconductor Switching in Melanins." *Science* 183 (4127): 853–855.

Meredith, P., and T. Sarna. 2006. "The Physical and Chemical Properties of Eumelanin." *Pigment Cell Research* 19 (6): 572–594. https://doi.org/10.1111/j.1600-0749.2006.00345.x.

Micillo, R., L. Panzella, K. Koike, G. Monfrecola, A. Napolitano, and M. d'Ischia. 2016. "'Fifty Shades' of Black and Red or How Carboxyl Groups Fine Tune Eumelanin and Pheomelanin Properties." *International Journal of Molecular Sciences* 17 (5): 746.

Migliaccio, L., P. Manini, D. Altamura, C. Giannini, P. Tassini, M. G. Maglione, C. Minarini, and A. Pezzella. 2019. "Evidence of Unprecedented High Electronic Conductivity in Mammalian Pigment Based Eumelanin Thin Films after Thermal Annealing in Vacuum." *Frontiers in Chemistry 7*:162. https://doi.org/10.3389/fchem.2019.00162.

Morresi, L., M. Ficcadenti, N. Pinto, R. Murri, M. Cuccioloni, M. Angeletti, and P. Tombesi. 2010. "Optical and Electrical Behavior of Synthetic Melanin Thin Films Spray-Coated." *Energy Procedia* 2 (1): 177–182.

Morris-Jones, R., B. L. Gomez, S. Diez, M. Uran, S. D. Morris-Jones, A. Casadevall, J. D. Nosanchuk, and A. J. Hamilton. 2005. "Synthesis of Melanin Pigment by *Candida albicans* In Vitro and during Infection." *Infection and Immunity* 73 (9): 6147–6150.

Morris-Jones, R., S. Youngchim, B. L. Gomez, P. Aisen, R. J. Hay, J. D. Nosanchuk, A. Casadevall, and A. J. Hamilton. 2003. "Synthesis of Melanin-Like Pigments by *Sporothrix schenckii* In Vitro and during Mammalian Infection." *Infection and Immunity* 71 (7): 4026–4033.

Mostert, A. B., P. Meredith, B. J. Powell, I. R. Gentle, G. R. Hanson and F. L. Prattd. 2016. "Understanding Melanin: A Nano-Based Material for the Future." In *Nanomaterials: Science and Applications*, ed. D. M. Kane, A. Micolich, and P. Roger, 175–202.New York: Jenny Stanford Publishing.

Mostert, A. B., B. J. Powell, I. R. Gentle, and P. Meredith. 2012. "On the Origin of Electrical Conductivity in the Bio-Electronic Material Melanin." *Applied Physics Letters* 100 (9): 093701.

Mostert, A. B., B. J. Powell, F. L. Pratt, G. R. Hanson, T. Sarna, I. R. Gentle, and P. Meredith. 2012. "Role of Semiconductivity and Ion Transport in the Electrical Conduction of Melanin." *Proceedings of the National Academy of Sciences* 109 (23): 8943–8947.

Motovilov, K. A., V. Grinenko, M. Savinov, Z. V. Gagkaeva, L. S. Kadyrov, A. A. Pronin, Z. V. Bedran, E. S. Zhukova, A. B. Mostert, and B. P. Gorshunov. 2019. "Redox Chemistry in the Pigment Eumelanin as a Function of Temperature Using Broadband Dielectric Spectroscopy." *RSC Advances* 9 (7): 3857–3867.

Nosanchuk, J. D., and A. Casadevall. 2006. "Impact of Melanin on Microbial Virulence and Clinical Resistance to Antimicrobial Compounds." *Antimicrobial Agents and Chemotherapy* 50 (11): 3519–3528. https://dx.doi.org/10.1128%2FAAC.00545-06.

Nosanchuk, J. D., R. E. Stark, and A. Casadevall. 2015. "Fungal Melanin: What Do We Know about Structure?" *Frontiers in Microbiology* 6:1463. https://dx.doi.org/10.3389%2Ffmicb.2015.01463.

Ordinario, D. D., L. Phan, W. G. Walkup IV, J. M. Jocson, E. Karshalev, N. Husken, and A. A. Gorodetsky. 2014. "Bulk Protonic Conductivity in a Cephalopod Structural Protein." *Nature Chemistry* 6 (7): 596–602.

Pal, A. K., D. U. Gajjar, and A. R. Vasavada. 2014. "DOPA and DHN Pathway Orchestrate Melanin Synthesis in Aspergillus Species." *Medical Mycology* 52:10–18.

Paulsen, B. D., K. Tybrandt, E. Stavrinidou, and J. Rivnay. 2020. "Organic Mixed Ionic–Electronic Conductors." *Nature Materials* 19:13–26.

Pradeep, F. S., and B. V. Pradeep. 2013. "Optimization of Pigment and Biomass Production from *Fusarium moniliforme* under Submerged Fermentation Conditions." *International Journal of Pharmacy and Pharmaceutical Sciences* 5:526–535.

R Core Team. 2013. *R: A Language and Environment for Statistical Computing*. Vienna, Austria: R Foundation for Statistical Computing. http://www.R-project.org/.

Rakitin, A., P. Aich, C. Papadopoulos, Y. Kobzar, A. S. Vedeneev, J. S. Lee, and J. M. Xu. 2001. "Metallic Conduction through Engineered DNA: DNA Nanoelectronic Building Blocks." *Physical Review Letters* 86:3670–3673.

Rakshit, T., and R. Mukhopadhyay. 2012. "Solid-State Electron Transport in Mn-, Co-, holo-, and Cu-Ferritins: Force-Induced Modulation is Inversely Linked to the Protein Conductivity." *Journal of Colloid and Interface Science* 388 (1): 282–292.

Rech, R., C. Cassini, A. Secchi, and M. A. Z. Ayub. 1999. "Utilization of Protein-Hydrolyzed Cheese Whey for Production of β-Galactosidase by *Kluyveromyces marxianus*. *Journal of Industrial Microbiology and Biotechnology* 23 (2): 91–96. https://doi.org/10.1038/sj.jim.2900692.

Riley, P. A. 1997. "Melanin." *The International Journal of Biochemistry & Cell Biology* 29 (11): 1235–1239.

Rižner, T. L., and M. H. Wheeler. 2003. "Melanin Biosynthesis in the Fungus *Curvularia lunata* (Teleomorph: *Cochliobolus lunatus*)." *Canadian Journal of Microbiology* 49 (2): 110–119. https://doi.org/10.1139/w03-016.

Roy, S., and J. W. Rhim. 2019. "Preparation of Carrageenan-Based Functional Nanocomposite Films Incorporated with Melanin Nanoparticles." *Colloids and Surfaces B: Biointerfaces* 176: 317–324.

Schmaler-Ripcke, J., V. Sugareva, P. Gebhardt, R. Winkler, O. Kniemeyer, T. Heinekamp, and A. A. Brakhage. 2009. "Production of Pyomelanin, A Second Type of Melanin, via the Tyrosine Degradation Pathway in *Aspergillus fumigatus*." *Applied Environmental Microbiology* 75 (2): 493–503.

Selvakumar, P., S. Rajasekar, K. Periasamy, and N. Raaman. 2008. "Isolation and Characterization of Melanin Pigment from *Pleurotus cystidiosus* (Telomorph of *Antromycopsis macrocarpa*)." *World Journal of Microbiology and Biotechnology* 24 (10): 2125–2131.

Sheliakina, M., A. B. Mostert, and P. Meredith. 2018. "Decoupling Ionic and Electronic Currents in Melanin." *Advanced Functional Materials* 28 (46): 1805514.

Siehr, D. J. 1981. "Melanin Biosynthesis in *Aureobasidium pullulans*." *Journal of Coating Technology* 53: 23–25.

Solano, F. 2014. "Melanins: Skin Pigments and Much More—Types, Structural Models, Biological Functions, and Formation Routes." *New Journal of Science* 2014:498276. https://doi.org/10.1155/2014/498276.

Takahashi, R., H. Wang, and J. P. Lewis. 2007. "Electronic Structures and Conductivity in Peptide Nanotubes." *Journal of Physical Chemistry B* 111 (30): 9093–9098.

Turick, C. E., A. A. Ekechukwu, C. E. Milliken, A. Casadevall, and E. Dadachova. 2011. "Gamma Radiation Interacts with Melanin to Alter its Oxidation-Reduction Potential and Results in Electric Current Production." *Bioelectrochemistry* 82: 69–73.

van der Pauw, L. J. 1958. "A Method of Measuring Specific Resistivity and Hall Effect of Discs of Arbitrary Shape." *Philips Research Reports* 13: 1–9.

Waleed Shinwari, M., M. Jamal Deen, E. B. Starikov, and G. Cuniberti. 2010. "Electrical Conductance in Biological Molecules." *Advanced Functional Materials* 20(12): 1865–1883.

Wang, Y., X. Wang, T. Li, P. Ma, S. Zhang, M. Du, W. Dong, Y. Xie, and M. Chen. 2018. "Effects of Melanin on Optical Behavior of Polymer: from Natural Pigment to Materials Applications." *ACS Applied Materials & Interfaces* 10 (15): 13100–13106.

Wickham, H. 2016. *ggplot2: Elegant Graphics for Data Analysis*. New York: Springer-Verlag.

Wunsche, J., Y. Deng, P. Kumar, E. Di Mauro, E. Josberger, J. Sayago, A. Pezzella, F. Soavi, F. Cicoira, M. Rolandi and C. Santato 2015. "Protonic and Electronic Transport in Hydrated Thin Films of the Pigment Eumelanin." *Chemistry of Materials* 27 (2): 436–442.

Appendix A: Current-Voltage Characteristic Curves of all Replicates and Test Configurations

Figure A-1. Current-voltage characteristic curves of synthetic melanin pellets for all test configurations and all replicates.

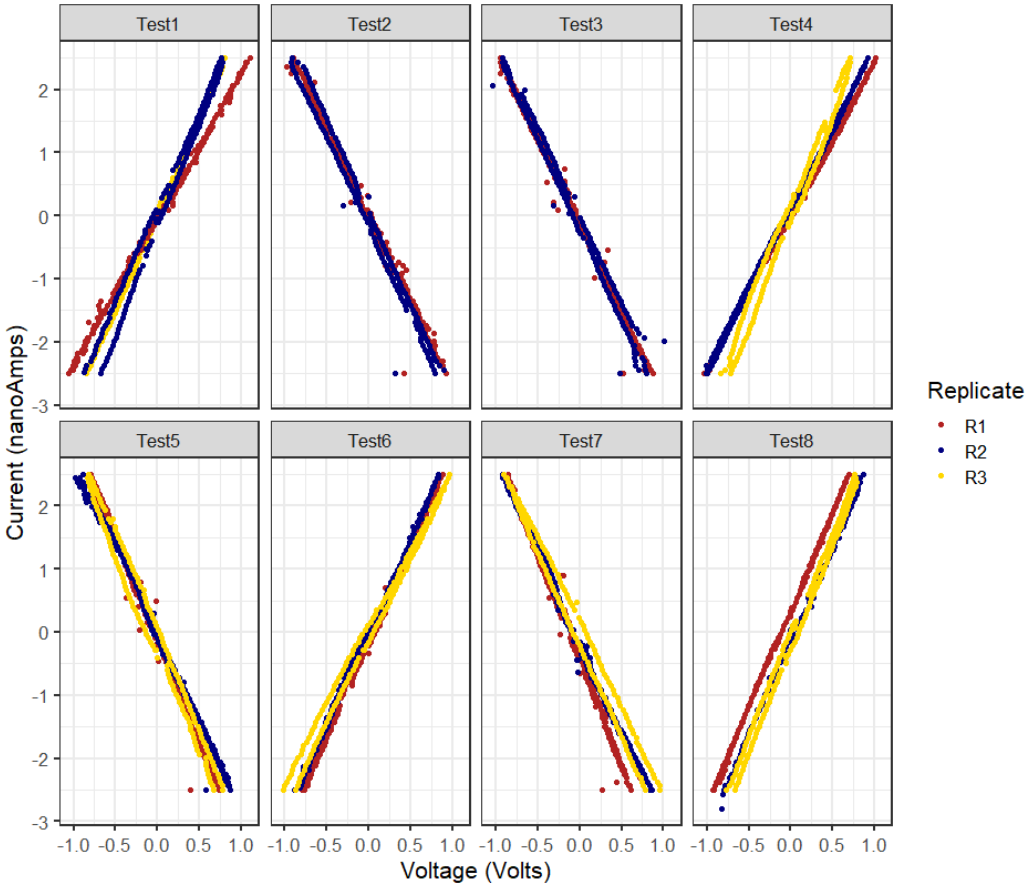

Figure A-2. Current-voltage characteristic curves of copperless *C. lunata* biomass for all test configurations and all replicates

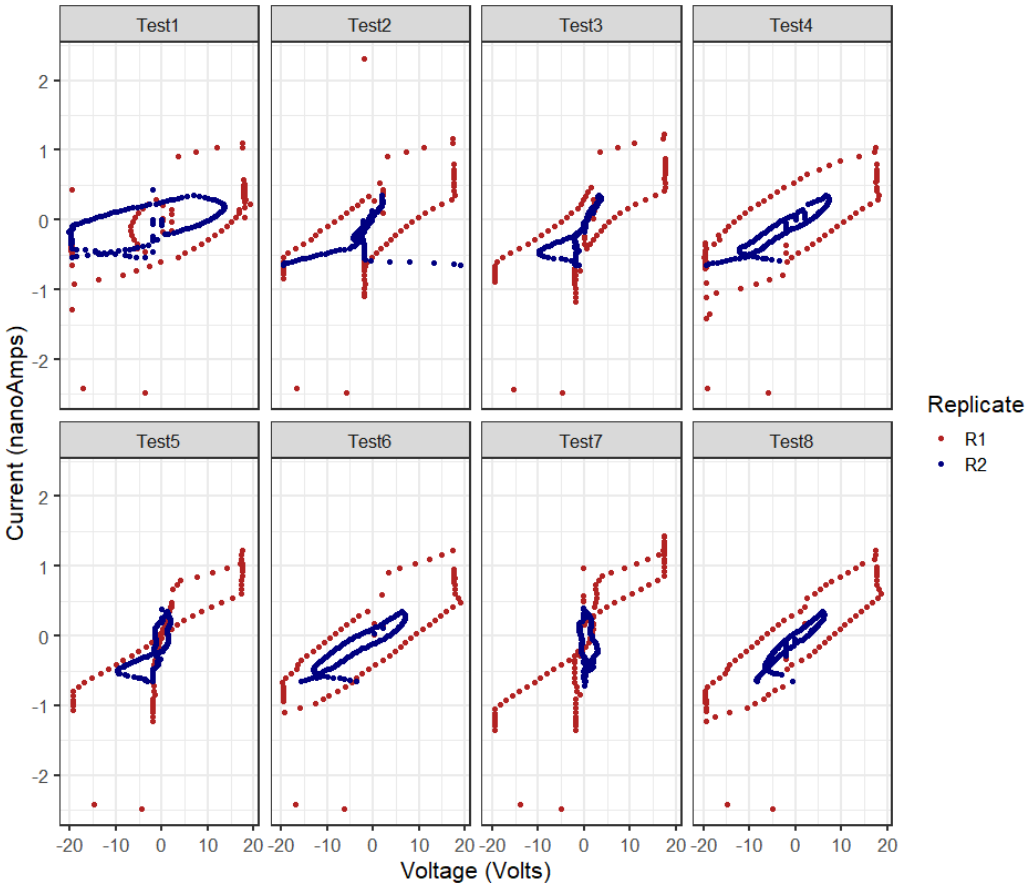

Figure A-3. Current-voltage characteristic curves of copper-doped *C. lunata* biomass for all test configurations and all replicates.

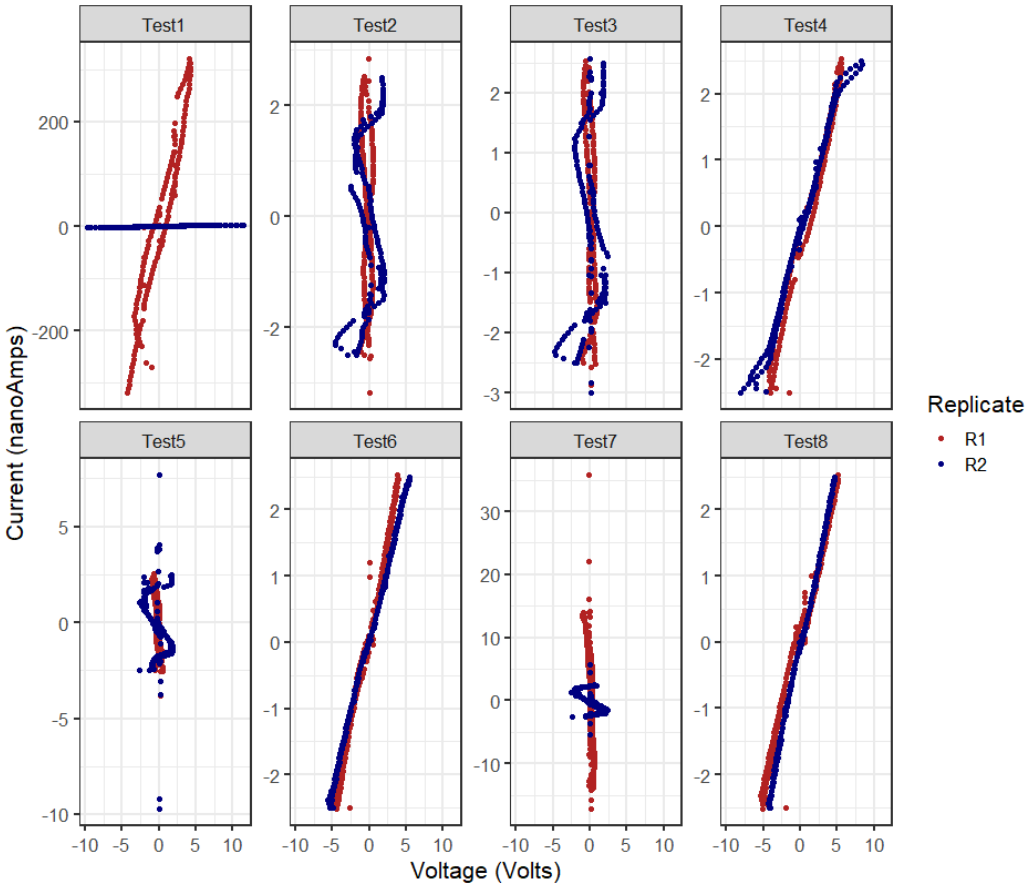

REPORT DOCUMENTATION PAGE

Form Approved
OMB No. 0704-0188

1. REPORT DATE (DD-MM-YYYY)	2. REPORT TYPE	3. DATES COVERED (From - To)
October 2020	Final / Technical Report	FY19–FY20

4. TITLE AND SUBTITLE

Evaluating the Conductive Properties of Melanin-Producing Fungus, *Curvularia lunata*, after Copper Doping

5a. CONTRACT NUMBER

5b. GRANT NUMBER

5c. PROGRAM ELEMENT

6. AUTHOR(S)

Robert M. Jones, Eftihia V. Barnes, Alison K. Thurston,and Robyn A. Barbato

5d. PROJECT NUMBER

5e. TASK NUMBER

5f. WORK UNIT NUMBER

7. PERFORMING ORGANIZATION NAME(S) AND ADDRESS(ES)

U.S. Army Engineer Research and Development Center
Cold Regions Research and Engineering Laboratory)
72 Lyme Road
Hanover, NH 03755-1290

U.S. Army Engineer Research and Development Center
Geotechnical and Structures Laboratory
3909 Halls Ferry Road
Vicksburg, MS 39180-6199

8. PERFORMING ORGANIZATION REPORT NUMBER

ERDC TR-20-25

9. SPONSORING / MONITORING AGENCY NAME(S) AND ADDRESS(ES)

Engineer Research and Development Center
3909 Halls Ferry Road
Vicksburg, MS 39180

10. SPONSOR/MONITOR'S ACRONYM(S)

ERDC

11. SPONSOR/MONITOR'S REPORT NUMBER(S)

12. DISTRIBUTION / AVAILABILITY STATEMENT

Approved for public release; distribution is unlimited.

13. SUPPLEMENTARY NOTES

Funded by Future Investment Fund, Funding Account Number U4373350

14. ABSTRACT

Melanins are pigmented biomacromolecules found throughout all domains of life. Of melanins' many unique properties, their malleable electrically conductive properties and their ability to chelate could allow them to serve as material for bioelectronics. Studies have shown that sheets or pellets of melanin conduct low levels of electricity; however, electrical conductance of melanin within a cellular context has not been thoroughly investigated. In addition, given the chelating properties of melanin, it is possible that introducing traditionally conductive metal ions could improve the conductivity.

Therefore, this study investigated the conductive properties of melanized cells and how metal ions change these. We measured the conductivity of pulverized *Curvularia lunata,* a melanized filamentous fungi, with and without the addition of copper ions. We then compared the conductivity measurements of the fungus to chemically synthesized, commercially bought melanin.

Our data showed that the conductivity of the melanized fungal biomass was an order of magnitude higher when grown in the presence of copper. However, it was two orders of magnitude less than that of synthetic melanin. Interestingly, conductance was measurable despite additional constituents in the pellet that may inhibit conductivity. Therefore, these data show promising results for using melanized cells to carry electrical signals.

15. SUBJECT TERMS

Applied mycology, Bioelectronics, Biomaterials, Conductivity, Copper ions, Current-voltage characteristics, Doping, Melanins, Metal binding

16. SECURITY CLASSIFICATION OF:			17. LIMITATION OF ABSTRACT	18. NUMBER OF PAGES	19a. NAME OF RESPONSIBLE PERSON
a. REPORT	b. ABSTRACT	c. THIS PAGE			19b. TELEPHONE NUMBER (include area code)
Unclassified	Unclassified	Unclassified	SAR	50	